Moscow-type *NN* potentials and three-nucleon bound states

V. I. Kukulin,[1,2] V. N. Pomerantsev,[1] Amand Faessler,[2] A. J. Buchmann,[2] and E. M. Tursunov[3]
[1]*Institute of Nuclear Physics, Moscow State University, 119899 Moscow, Russia*
[2]*Institute for Theoretical Physics, University of Tübingen, Auf der Morgenstelle 14, D-72076 Tübingen, Germany*
[3]*Institute of Nuclear Physics Academy of Sciences, Tashkent, Uzbekistan*
(Received 31 July 1997)

A detailed description of Moscow (M)-type potential models for the *NN* interaction is given. The microscopic foundation of these models, which appear as a consequence of the composite quark structure of nucleons, is discussed. M-type models are shown to arise naturally in a coupled channel approach when compound or bag-like six-quark states, strongly coupled to the *NN* channel, are eliminated from the complete multiquark wave function. The role of the deep-lying bound states that appear in these models is elucidated. By introducing additional conditions of orthogonality to these compound six-quark states, a continuous series of almost on-shell equivalent nonlocal interaction models, characterized by a strong reduction or full absence of a local repulsive core (M-type models), is generated. The predictions of these interaction models for $3N$ systems are analyzed in detail. It is shown that M-type models give, under certain conditions, a stronger binding of the $3N$ system than the original phase-equivalent model with nodeless wave functions. An analysis of the $3N$ system with the new versions of the Moscow *NN* potential describing also the higher even partial waves is presented. Large deviations from conventional *NN* force models are found for the momentum distribution in the high momentum region. In particular, the Coulomb displacement energy $E_B(^3\mathrm{He})-E_B(^3\mathrm{H})$—when $E_B(^3\mathrm{H})$ is extrapolated to the experimental value displays a promising agreement with experiment: $\Delta E_C \simeq 740$ KeV. The validity and limits of two-body *NN* potentials in nuclei is discussed in the light of our analysis. [S0556-2813(98)02402-9]

PACS number(s): 13.75.Cs, 21.45.+v, 21.10.Sf, 24.90.+d

I. INTRODUCTION

It has been known for a long time that standard *NN* interaction models based on one-meson exchange [1–5], meet significant difficulties in explaining standard properties of few-nucleon systems, ordinary nuclei, as well as nuclear matter [2,3]. In a number of cases, difficulties arise even in the well investigated area of low energies ($\sim 3-10$ MeV) [6–8]. In order to reach agreement between theory and experiment for some key observables (binding energy, magnetic moments, etc.) $3N$ forces and meson-exchange currents (MEC) are very often introduced. However, in practical applications, the values of cutoff masses are sometimes incompatible with those used in the initial two-body interaction model [2].

These discrepancies have resulted in a revival of interest in nonlocal nuclear force models (see, e.g., [9,10]). The latter give predictions closer to experiment than those of conventional local models [9]. In fact, from the viewpoint of the more fundamental level of quantum chromodynamics (QCD) and the quark model, the *NN* interaction must be strongly nonlocal at small distances [11,12] due to quark exchanges between the nucleons (three-quark clusters) [11–13]. A number of nonlocal models for the *NN* interaction, either phenomenological [14,15] or microscopic [11,13,16–19], including both meson and quark degrees of freedom have already been suggested. However, most of them lead to rather complicated and bulky momentum-dependent *NN* interaction operators that can hardly be used for practical calculations in nuclear many-body systems. This explains the lack of *qualitative* studies of the structure of few-nucleon systems using quark degrees of freedom. Such studies would be extremely important for nuclear physics in general.

Therefore, it is a rather urgent to develop a simple *NN*-interaction model which *simultaneously* takes into account both meson and quark degrees of freedom, and which is applicable to few- and many-nucleon systems. Having at our disposal a reasonably simple and realistic *NN* interaction model of the above hybrid type, we can study its qualitative and quantitative consequences in the many-body problem.

The purpose of this work is to do just that. At first, we develop a simple nonlocal *NN* interaction model that is based on the quark structure of the nucleon. We then study its predictions for the three-body bound state problem and compare these predictions with those of conventional force models. An additional argument in favor of our approach is that quark degrees of freedom are not explicitly seen in the energy region ($E_{\mathrm{lab}}^{NN} \leqslant 300$ MeV). Only rather indirect signals of these hidden degrees of freedom can be studied. One such indirect quark effect considered in the present work is the internal fermization of the nuclear wave functions [20]. Such an ''internal'' fermization changes the wave function of the system mainly, but not exclusively, at small distances and leads to the occurrence of additional internal nodes in the wave functions at about the same place where the repulsive core of conventional force models is situated.

From a formal point of view, the elimination of quark degrees of freedom results in additional orthogonality conditions for the *NN* channel in conformity with the classical Feshbach method for projecting onto mutually orthogonal channels [21]. As a result, the orthogonality constraints lead to additional internal nodes in the wave functions [22,23]. Therefore, the height of the local repulsive core can be strongly reduced (see Secs. III and IV). We emphasize that a

 © 1998 The American Physical Society

large part of the repulsion in lowest partial waves is not due to the local core produced by vector meson (ω and ρ) exchange but comes from these additional orthogonality conditions. As will become clearer later on, this leads to a substantial increase of the average nucleon kinetic and potential energy, which in turn has numerous consequences for the structure of the nucleus. Below we point out only the most important differences between conventional nuclear force models and Moscow (M)-type models.

Because of the additional orthogonality constraints, the strength of the repulsive core, mainly due to ω-meson exchange, can be considerably reduced down to values, dictated by SU(3) symmetry [2], i.e., $g^2_{\omega NN}/4\pi \sim 5$. As a result, the attractive part of the potential is considerably deeper than that of conventional force models. However, this does not cause any discrepancy with experiment because the additional orthogonality conditions lead to an effective reduction of the local attraction at intermediate distances.

Due to the sharp increase of kinetic energies in the NN channel at small distances $r_{NN} < 1$ fm, the *relative* importance of nonlocal and energy-dependent terms in the NN interaction operator coming from meson retardation effects [2] or $6q$ bags are strongly suppressed. As a result, all complicated and nonstatic short-range nonlocalities originating from different sources are replaced by a very simple nonlocal *separable* potential. This nonlocal separable potential has the form of a projection operator and effectively describes the additional orthogonality conditions [24]. This allows us to drastically simplify the description of the NN interaction, especially at small internucleon distances.

An important difference is also the *local* character of the deep attractive potential which is universal for all partial waves. This universality can be interpreted as a consequence of pseudoscalar π, η, and scalar σ exchanges between nucleons. Here, the scalar σ-exchange, gives a strong attraction (depth ~ 500 MeV [11]) between nucleons at intermediate distances.

For sake of brevity, we shall call NN-force models, which are characterized by (i) a strongly reduced local repulsive core (or even by the full absence of it), (ii) a strong attraction in the intermediate range and additional orthogonality conditions, as Moscow-type models. For a substantiation of these models it is important to recall the following relatively new results.

In a number of recent studies [25,26] it was established that a limiting case of such models, which does not include any repulsive core at all, nearly coincides with the supersymmetric (SUSY) partner of the Reid-soft-core (RSC) potential. Thus, both types of interaction models, conventional force models with a local repulsive core and M-type force models, are related by purely algebraic symmetry transformations. For a pedagogical discussion of this point see Ref. [27].

Recently Nakaichi-Maeda [28] has found that the phenomenological separable NN potential of Tabakin [29], leading to internal nodes in the radial deuteron and NN-scattering wave functions, is a simple unitary-pole approximation (UPA) to the above Moscow NN potential, i.e., in the UPA-approach both models coincide with high accuracy.

These results, established by independent groups, are not accidental; rather they are indicative of the quark dynamics underlying the Moscow NN potential. One of the main purposes of the present work is to explain this in greater detail and to study the qualitative behavior of M-type NN interaction models in the nuclear three-body problem.

This work is organized as follows. In Sec. II we provide a substantiation of M-type models within the framework of the quark model. Section III presents a pedagogicial introduction to the main physical ideas underlying the Moscow model. We study a simple scalar interaction and investigate its qualitative predictions for the three-nucleon bound state. Section IV discusses the more complete model including tensor forces for positive parity partial waves. In Sec. V these more realistic models are applied to the three-nucleon bound-state problem. We emphasize the important contribution of the tensor force to the $3N$ binding energy. The interference of central and tensor forces inherent in these models is quite different from conventional force models. The differences in predictions between traditional force models and M-type models are pointed out. In the conclusion our main findings are summarized.

II. ORIGIN OF NN INTERACTION MODELS WITH ADDITIONAL ORTHOGONALITY CONDITIONS: M-TYPE MODELS

A. Six-quark permutational symmetries and the NN interaction

Consider a two-nucleon system that is described in the framework of the nonrelativistic quark model [12,13]. The quark Hamiltonian H consists of the following components:

$$H = H_0 + V_{\rm OGE} + V_{\rm conf} + V_{\rm OME}, \tag{1}$$

where $H_0 = \Sigma_{i=1}^{6}[m_i + p_i^2/(2m_i)]$ is the kinetic energy of the $6q$ system. The interaction $V_{\rm OGE}$ accounts for one-gluon exchange, and the confinement interaction $V_{\rm conf}$ takes the standard form [11,13]. In the one-meson exchange potential between quarks $V_{\rm OME}$ we include, as usual, π- and σ-meson exchange potentials [13,18].

The totally antisymmetric (denoted by subscript A) wave function $\Psi_A(x_1, \ldots, x_6)$ can be expanded into a sum of irreducible representations (IR) of the symmetry group S_6 [30,31]. The sum extends over all allowed IR of the symmetry group S_6, characterized by Young schemes $[f]$, that lie in the outer product space $S_3 \otimes S_3$:

$$\Psi_A(x_1, \ldots, x_6) = \frac{1}{\sqrt{n_f}} \sum_{[f]r} \Phi([f]r; \vec{r}_1, \ldots, \vec{r}_6)\chi_{CST}([\tilde{f}]\tilde{r}), \tag{2}$$

where the coordinates $x_1, \ldots, x_6$ collectively stand for the position, and the spin, isospin, and color quantum numbers of the six quarks. Here, $\Phi([f]r; \vec{r}_1, \ldots, \vec{r}_6)$ is the orbital part of the total six-quark wave function, and $\chi_{CST}([\tilde{f}]\tilde{r})$ is its color-spin-isospin part. The Young scheme of the space part of the six-quark wave function is denoted by $[f]r$, where r is the corresponding Yamanouchi symbol. The Young scheme $[\tilde{f}]\tilde{r}$ stands for the unique irreducible representation in spin-isospin-color space which is adjoint to $[f]r$. For brevity we omit the Young symbols $[f]_C$, $[f]_S$, $[f]_T$,

relating separately to the color, spin and isospin parts of the function χ_{CST}. Furthermore, n_f is the dimension of the IR corresponding to the Young scheme $[f]$.

One can easily see that, according to the Littlewood theorem [31], the allowed Young schemes, which describe the permutational symmetry of six-quark orbital (X) wave functions $\Phi([f]r)$, are

$$[3]_X \times [3]_X = [6]_X + [42]_X + [51]_X + [33]_X , \tag{3}$$

where the first two terms correspond to even orbital angular momenta (with positive parity), and the last two terms to odd orbital angular momenta (with negative parity) of the relative NN wave function. Thus, for even partial waves in the relative NN wave function, the allowed space symmetries are $[6]_X$ or $[42]_X$, whereas for odd ones, they are $[51]_X$ or $[33]_X$. Using the two-center shell model basis with distance R between the two centers, one can show [32] that all allowed six-quark wave functions of the type $|S_+^3 S_-^3 [f] LST\rangle$ approach the usual shell model configurations $|s^m p^n [f] LST\rangle$ $(m+n=6)$ in the limit $R \to 0$. Thus, the NN state with the totally symmetric Young scheme $[f]_X = [6]_X$ corresponds to the six-quark state $|s^6 [6]_X [2^3]_{CS} L=0, ST\rangle$ while the NN state with mixed symmetry configuration $[42]_X$ corresponds to a six-quark state with two excited p-shell quarks:

$$|s^4 p^2 [42]_X [f]_{CS} L=0, ST\rangle,$$

where $[f]_{CS} = [42],[321],[2^3],[31^3],[24^4]$ are the possible Young schemes appearing in the Clebsch-Gordan decomposition of the internal product $[2^3]_C [42]_S$.

In a series of works by many different authors [13,16,33–35], it was shown that, with a quark Hamiltonian of the form of Eq. (1), the excited six-quark configurations $|(0s)^5 (1s) [42]_X\rangle$ and $|(0s)^4 (0p)^2 [42]_X\rangle$ which are compatible with S-wave relative NN motion, are admixed with large weights to the fully symmetric six-quark configuration $|(0s)^6 [6]_X\rangle$. The color-magnetic term $\sim \boldsymbol{\lambda}_i \cdot \boldsymbol{\lambda}_j \, \boldsymbol{\sigma}_i \cdot \boldsymbol{\sigma}_j$ is mainly responsible for this. Thus, in lowest partial waves of the relative NN wave function, there is a superposition of two different $6q$-space symmetries: the fully symmetric $|(0s)^6 [6]_X\rangle$ and the mixed symmetric $|(0s)^4 (0p)^2 [42]_X\rangle$ for S waves, and similarly the $|(0s)^5 (0p) [51]_X\rangle$ and $|(0s)^3 (0p)^3 [33]_X\rangle$ for P waves. It is important to remark that the above superpositions include the excited $p_{3/2}$ single-quark states.

In recent work [13], it was shown that six-quark components with different space symmetries play a very different role in the NN interaction. For example, the totally symmetric six-quark components $|(0s)^6 [6]_X\rangle$ are projected onto the NN cluster channel with rather *small weights*, whereas they have large projections onto the $\Delta\Delta$ and hidden-color channels. In contrast, the mixed symmetry components $|s^4 p^2 [42]_X\rangle$ (in S waves) have *large* projections onto both the cluster NN channel and the nucleon-isobar channels $N_1^* N_2^*$.

Thus, there is a natural separation of the complete six-quark wave function into two mutually orthogonal parts of a different physical nature:

$$\Psi_A = \Psi_{6q} + \Psi_{\rm clust} , \tag{4}$$

where Ψ_{6q} is the baglike component, which can be constructed from square integrable functions φ_i corresponding to various six-quark bag states. These are the states with maximal space symmetry, i.e., s^6 for relative S waves and $s^5 p$ for relative P waves:

$$\Psi_{6q} = \sum_{i=1}^{N} C_i \varphi_i , \tag{5}$$

where N is the number of six-quark states. For the cluster component we use the standard resonating group method (RGM) ansatz

$$\Psi_{\rm clust}(\boldsymbol{\xi}_1, \boldsymbol{\xi}_2, \mathbf{R}) = \mathcal{A}\{\varphi_N(\boldsymbol{\xi}_1) \varphi_N(\boldsymbol{\xi}_2) \widetilde{\chi}(\mathbf{R})\}, \tag{6}$$

where $\mathcal{A}$ is the antisymmetrizer with respect to the six quarks. Here, $\varphi_N(\boldsymbol{\xi}_i)$ is the three-quark wave function of a single nucleon where the internal coordinates are collectively denoted by $\boldsymbol{\xi}_i$, and $\widetilde{\chi}(\mathbf{R})$ is the relative motion wave function of two three-quark clusters.

B. Two-phase model for the NN interaction

Our approach differs from the majority of hybrid NN interaction models which are also based on a decomposition of the form of Eq. (4). In contrast to, for example, the quark compound bag (QCB) model by Simonov [14], we require the mutual orthogonality of the components Ψ_{6q} and $\Psi_{\rm clust}$:

$$\langle \Psi_{6q} | \Psi_{\rm clust} \rangle = 0. \tag{7}$$

Moreover, we require that the cluster component be orthogonal to all baglike states φ_i from which the component Ψ_{6q} is constructed:

$$\langle \varphi_i | \Psi_{\rm clust} \rangle = 0, \quad i = 1, \ldots, N. \tag{8}$$

When combined with Eqs. (4)–(6), this leads to corresponding orthogonality conditions for the RGM relative motion function $\widetilde{\chi}(R)$:

$$\langle g_i | \widetilde{\chi} \rangle = 0, \quad i = 1, \ldots, N, \tag{9}$$

where

$$g_i(\mathbf{R}) = \langle \varphi_i(\boldsymbol{\xi}_1, \boldsymbol{\xi}_2, \mathbf{R}) | \varphi_N(\boldsymbol{\xi}_1) \varphi_N(\boldsymbol{\xi}_2) \rangle \tag{10}$$

are projections of six-quark baglike functions onto the NN channel. To emphasize the importance of orthogonality conditions in our approach we put a tilde over the relative motion wave function χ. We point out that a similar model with mutually orthogonal $6q$ and NN channels in configuration space has been suggested by Lomon [19]. The model of Lomon is similar in spirit to our model but different in realization. It is obvious that at intermediate and large distances, where the clusterlike components dominate, the NN dynamics should be rather well described by a meson-exchange [one-boson-exchange (OBE) and two-pion exchange (TPE)] model. Explicit quark and gluon degrees of freedom are unimportant here. On the contrary, in the short-distance regime, with maximal overlap of the nucleon wave functions, explicit quark-gluon degrees of freedom, described by the compound

states φ_i should play a decisive role. In this way we arrive at what could be called a *duality principle* for the baryon-baryon interaction which can be formulated as follows. The total six-quark wave function naturally separates into two mutually orthogonal (i.e., nonoverlapping) components.

One component has a three-quark cluster structure where the baryons (including isobars) can be considered as separate entities, and where the dominant dynamical mechanism is meson exchange between the clusters, while the quark-gluon degrees of freedom are only of minor significance.

The other component has a six-quark bag structure. Its dynamics is governed by explicit quark-gluon degrees of freedom. This component is sensitive to, for example, the particular form of confinement, the value of the scalar quark condensate $\langle q\overline{q}\rangle$, etc., and depends only weakly on the ''external'' meson dynamics.

Therefore, when constructing a proper NN interaction potential, the baglike components should be somehow excluded from the very beginning, because these components are very hard to describe by any reasonable NN potential. For this component one should use a different formalism. This is in complete analogy to the optical potential model in nuclear physics, which is not at all applicable in situations, where the nucleon-nucleus scattering proceeds via isolated compound-states of the nucleus. In this analogy the optical nucleon-nucleus potential corresponds to the meson exchange dynamics between nucleons while the nucleon-nucleus compound states correspond to the six-quark bags in NN scattering.

Projecting the total six-quark Schrödinger equation

$$H\Psi = E\Psi$$

onto the six-quark states φ_i and onto the NN cluster channel we obtain, using the orthogonality conditions (8), the following set of coupled equations:

$$\left\{ \begin{array}{l} \sum_j (\hat{H}_{ij} - E\delta_{ij}) C_j + \langle f_i | \widetilde{\chi}\rangle = 0, \qquad (11) \\ \sum_j C_j f_j + (\hat{\mathcal{H}}^{\rm RGM} - E\hat{\mathcal{N}})\widetilde{\chi} = 0. \qquad (12) \end{array} \right\}$$

Here, we have introduced the following abbreviations:

$$\hat{H}_{ij} = \langle \varphi_i | H | \varphi_i \rangle, \qquad (13)$$

$$f_i(\mathbf{R}) = \langle \varphi_i | H | \varphi_N \varphi_N \rangle. \qquad (14)$$

$\hat{\mathcal{H}}^{\rm RGM}$ and $\hat{\mathcal{N}}$ are integral operators with kernels

$$\mathcal{H}^{\rm RGM}(\mathbf{R},\mathbf{R}') = \langle \varphi_N \varphi_N | H\mathcal{A} | \varphi_N \varphi_N \rangle, \qquad (15)$$

$$\mathcal{N}(\mathbf{R},\mathbf{R}') = \langle \varphi_N \varphi_N | \mathcal{A} | \varphi_N \varphi_N \rangle. \qquad (16)$$

Solving the linear algebraic equations (11) with respect to the coefficients C_i and substituting its solution

$$C_i = \sum_j (E - \hat{H})^{-1}_{ij} \langle f_i | \widetilde{\chi}\rangle \qquad (17)$$

into Eq. (12), we find the equation of motion for the NN relative wave function $\widetilde{\chi}$:

$$\left(\hat{\mathcal{H}}^{\rm RGM} - E\hat{\mathcal{N}} + \sum_{ij} |f_i\rangle (E - \hat{H})^{-1}_{ij} \langle f_i| \right) \widetilde{\chi} = 0. \qquad (18)$$

This equation must be solved together with the additional orthogonality conditions (9). After that one can calculate the coefficients C_i via Eq. (17) and hence the total wave function Ψ. Equation (18) constitutes our two-phase model for the NN interaction.

Due to the appearance of the norm kernel $\mathcal{N}$, the RGM relative motion wave function $\widetilde{\chi}$ in Eq. (18) cannot yet be interpreted as the probability amplitude for finding the nucleons at a relative distance R. In order to obtain a NN relative motion wave function that can be interpreted in the usual sense, we define a renormalized function $\hat{\widetilde{\chi}} = \mathcal{N}^{1/2}\widetilde{\chi}$ and a corresponding effective nucleon-nucleon interaction

$$(T_R + V_{\rm eff} - E)\hat{\widetilde{\chi}} = 0, \qquad (19)$$

where

$$V_{\rm eff} = \mathcal{N}^{1/2}\hat{\mathcal{H}}^{\rm RGM}\mathcal{N}^{1/2} - T_R + \sum_{ij} |\hat{f}_i\rangle (E - \hat{H})^{-1}_{ij} \langle \hat{f}_i|, \qquad (20)$$

$$\hat{f}_i = \hat{\mathcal{N}}^{1/2} f_i .$$

The effect of the overlap kernel $\mathcal{N}(\mathbf{R},\mathbf{R}')$ for the NN system can be reasonably well approximated by the expression [13]

$$\mathcal{N}(\mathbf{R},\mathbf{R}') \simeq \frac{1}{10}\delta(\mathbf{R} - \mathbf{R}'), \qquad (21)$$

which differs from the usual local NN potential just by a combinatorial factor. Thus, the effective interaction can be cast into the form

$$V_{\rm eff} = V_{\rm dir} + V_{\rm ex} + V_{NqN}, \qquad (22)$$

where $V_{\rm dir}$ is the direct (folding) potential, including one-meson exchanges between three-quark clusters only, i.e., the one-meson-exchange nucleon-nucleon potential. Because the one-gluon exchange operator is diagonal with respect to quark permutations between nucleons it does not contribute to $V_{\rm dir}$. $V_{\rm ex}$ is the nonlocal short-range exchange potential, and V_{NqN} is an effective potential due to the coupling of NN and $6q$ channels:

$$V_{NqN} = 10 \sum_{ij} |f_i\rangle (E - \hat{H})^{-1}_{ij} \langle f_j|. \qquad (23)$$

The effective two-nucleon Schrödinger equation for the orthogonalized and renormalized relative motion wave function $\widetilde{\chi}(R)$:

$$\left\{ \begin{array}{l} (T_R + V_{\rm dir} + V_{\rm ex} + V_{NqN} - E)\hat{\widetilde{\chi}} = 0 \\ \langle g_i | \hat{\widetilde{\chi}}\rangle = 0, \qquad i = 1, \ldots, N \end{array} \right. \qquad (24)$$

provides the basis for the justification of NN-interaction models of Moscow type.

The main point is that the solution of Eq. (24) is defined only in the *subspace orthogonal* to the functions g_i. Due to this orthogonality requirement, we inevitably introduce nodes in the NN scattering wave functions at small distances [22,23,33–36]. The node positions are very stable as the NN scattering energy E is increased [13,22]. This behavior of scattering wave functions can be quite naturally formulated in the language of interaction potentials that have a very deep attractive well ($\sim$1 GeV) [23] with additional deeply-lying bound states. In fact, compared to the deep attractive well with $|V_0| \approx 1$ GeV, the relative scattering energy E is negligible. Therefore, the position of the innermost node $r_{\rm node}$ is basically determined by the well depth V_0:

$$\sqrt{m_N\,(E-V_0)}\; r_{\rm node} \approx \sqrt{m_N\,|V_0|}\; r_{\rm node} \approx \pi.$$

Thus, the inner node of the scattering wave function is almost stationary for center of mass energies up to $\sim$2 GeV in the laboratory frame in nonrelativistic kinematics. Inserting the numerical values for the nucleon mass, and V_0 we find that the stationary node is located at $R_n \simeq 0.6$ fm in the case of relative S waves ($R_n \simeq 0.9$ fm in the case of P waves). We point out that this node plays the role of the repulsive core in the NN interaction.

Because the nodal solutions of the basic equation (24) with orthogonality conditions correspond to very large kinetic energies, the short-range nonlocal potential $V_{\rm ex}$, which includes the quark exchange diagrams, plays only a minor role in the subspace of nodal wave functions. This is in analogy to the nuclear orthogonality condition model (OCM) of Saito [36]. Therefore, $V_{\rm ex}$ can be omitted from Eq. (24) in good approximation.

Finally, we take the last step in the substantiation of the model. In absence of the vector (ρ and ω) meson contribution in the total Hamiltonian (1), the meson-exchange potential $V_{\rm dir}$ in Eq. (24) corresponds to π- and σ-meson exchange. Therefore, it is strongly attractive with a depth of the central potential of about $\sim$500 MeV. Together with the nonlocal attractive (for $E < E_1$) part V_{NqN}, it results in an *effective* deep ($\sim$1 GeV) attractive potential, which was found in our initial attempts [23], and has since been justified [13,22,27,37] within the framework of the quark model. In fact, we have found out only quite recently [38] that the combination of the local attractive σ-meson exchange potential (with a depth of about 500 MeV) and the nonlocal attraction V_{NqN}, representing the coupling of the NN and $6q$-baglike channels, is exactly phase-shift equivalent to the deep ($\sim$1 GeV) effective *attractive* potential of M type.

The Moscow potential is the simplest local model, which ensures the orthogonality of its solutions to a function φ_0 that approximately describes the projection of the fully symmetric $(0s)^6$ six-quark state onto the NN channel (in S waves). We emphasize that the occurrence of unobservable deep-lying bound states in Eq. (24) poses no problem, because the equation for the NN channel wave function is considered in the appropriate subspace of nodal wave functions, which is *orthogonal* to the nodeless bound states. Additional extra deeply bound states arise only in the solution of the appropriate Schrödinger equation in the *complete* space.

In order to understand the reasons for the occurrence of deep-lying bound states, it is very instructive to recollect [13] that, the weight of the NN configuration (with *unexcited* nucleons) in symmetric baglike six-quark states $|s^6[6]_X[2^3]_{CS} L=0,ST\rangle$ is very small; whereas the weight of the $\Delta\Delta$ channel is appreciably larger and the main contribution comes from hidden color CC channels, whose wave functions are localized (because of confinement) at small distances [39]. As a result of the strong coupling of the initial NN channel and the baglike six-quark channels, the probability for finding an NN configuration with unexcited nucleons vanishes almost completely at small distances.[1] Thus, at very small distances, where the extra deeply bound states are localized, there is basically no nucleon-nucleon configuration. In this regime, the $2N$ system can be viewed as though ''being dissolved'' in a quark ''soup.'' Remembering the Cheshire Cat smile, it is appropriate to name these deeply-lying bound states ''Cheshire-Cat bound states (CCBS).''

In applications of the model to many-nucleon systems, it should be kept in mind that the Moscow potential describes in an effective way the single-channel system, i.e., the $2N$ system with *unexcited* nucleons, while the real $2N$ system should be described by the above two-component model. Thus the description of three-nucleon systems given by the Moscow *potential* model must be supplemented with an additional $6q+N$ contribution which is expected to be strongly *attractive*. Before we discuss the Moscow NN potential in greater detail, we explain the main ideas of our approach within the framework of a simple toy model.

III. A SIMPLE M-TYPE MODEL FOR THE NN INTERACTION

A. General considerations

In this section we compare two alternative models for the NN interaction. For clarity, we use the simplest possible example, i.e., two spinless nucleons interacting via a scalar potential $V(r)$:

$$V(r) = g_R\, V_R(r) + g_A\, V_A(r). \tag{25}$$

The potential includes a short-range repulsive core $g_R\, V_R(r)$, and a long-range attraction $g_A\, V_A(r)$. The coupling constants g_R and g_A are chosen such that the system has a single bound state with energy ε_0 (''deuteron'') and scattering phase shifts $\delta_l(E)$, $l=0,1,\ldots$.

Let us try to find a modified potential $V'(r) = g'_R\, V_R(r) + g_A\, V_A(r)$ with a reduced strength of the repulsive core, but simultaneously introduce an additional constraint that ensures the orthogonality of the solution of the Schrödinger equation to some function φ_0 localized in the core area:

$$\begin{cases} (T_r + V'(r) - \varepsilon)\,\widetilde{\psi}(r) = 0, & \text{(26a)} \\ \langle \varphi_0 | \widetilde{\psi}(r) \rangle = 0. & \text{(26b)} \end{cases}$$

[1] A similar conclusion concerning the suppression of the NN channel in favor of the $\Delta\Delta$ and other isobar channels can possibly be derived in a formalism based on meson Lagrangians [40] without any reference to the quark model.

The physical meaning of the additional orthogonality constraint has already been discussed and partly been elucidated above. Here, we consider this orthogonality condition as a formal constraint that the solution has to satisfy.

Equation (26a) with the additional condition (26b) can be rewritten in the form of a single equation with the nonlocal interaction (see [36])

$$[T_r+V'(r)-\varepsilon]|\widetilde{\psi}(r)\rangle=|\varphi_0\rangle\langle\varphi_0|T_r+V'(r)|\widetilde{\psi}(r)\rangle. \tag{27}$$

The solutions of this equation are, as one can easily see, orthogonal to φ_0 for any $\varepsilon\neq 0$. Only for $\varepsilon=0$, the required orthogonality is not guaranteed and Eq. (27) gives an incorrect behavior for the corresponding off-shell t matrix.

One can apply a more convenient approach, known as the method of orthogonalizing pseudopotentials (OPP) [24]. In this approach, the additional orthogonality condition (26b) is taken into account via the projection operator $\Gamma=|\varphi_0\rangle\langle\varphi_0|$ which projects onto the ''forbidden'' subspace with a large coupling constant μ:

$$(T_r+V'(r)+\mu|\varphi_0\rangle\langle\varphi_0|-\varepsilon)|\widetilde{\psi}_\mu(r)\rangle_{\mu\to\infty}=0. \tag{28}$$

In our example, the forbidden subspace is just a one-dimensional subspace spanned by the vector φ_0. In the limit $\mu\to\infty$, the solutions of Eq. (28) $\widetilde{\psi}_\mu(r)$ have been shown [24] to be rigorously orthogonal to φ_0, i.e.,

$$\lim_{\mu\to\infty}\langle\varphi_0|\widetilde{\psi}_\mu\rangle=0.$$

For $\varepsilon\neq 0$ the solution $\widetilde{\psi}_\mu$ coincides with the solution of the Saito equation (27). The projection operator $\Gamma=|\varphi_0\rangle\langle\varphi_0|$defines a ''forbidden'' subspace $\mathcal{H}_\Gamma$ of the full two-particle Hilbert space $\mathcal{H}$ which can be decomposed as

$$\mathcal{H}_\Gamma\oplus\mathcal{H}_Q=\mathcal{H},$$

where $\mathcal{H}_Q$ is the orthogonal complement to $\mathcal{H}_\Gamma$.

Thus, we consider the problem of finding a modified potential $V'(r)$ that is phase-shift equivalent to the initial potential $V(r)$ of Eq. (25) and which has the bound state at the same energy ε_0 in the *subspace* $\mathcal{H}_Q$ orthogonal to φ_0. For an arbitrary φ_0, rigorous solutions of such an inverse scattering problem are, to our knowledge, not available. Therefore, we search for approximate solutions. In order to further elucidate the relation of M-type models and conventional *NN* force models, we are interested in such solutions that contain a repulsive core that is weaker than that in the initial potential $V(r)$. Although the modified potential $V'(r)$ becomes deeper when the core is weakened, the introduction of the additional orthogonality constraint of Eq. (26b) renders the Hamiltonian *effectively* weaker. Due to this compensation, both the phase shifts and the bound state energies remain the same, albeit with some error.

On the other hand, if we use the OPP method [24,36] the modified pseudopotential has the form

$$\widetilde{V}'(r)\underset{\mu\to\infty}{=}V'(r)+\mu|\varphi_0\rangle\langle\varphi_0|. \tag{29}$$

Using this method, it is possible to work *in the total* space instead of only in the subspace. This is one of the practical advantages of the OPP method. Thus, in the OPP approach, a part of the *local* short-range repulsion is replaced by a separable repulsive potential with an infinite coupling constant μ (29). If φ_0 is a bound-state solution of the potential $V'(r)$, the potentials V' and $\widetilde{V}'$ are completely phase-shift equivalent. For this case, the solution of the inverse problem, i.e., the transition to a phase-shift equivalent potential with a local repulsive core *without* a deep-lying bound state, is well known. This is a supersymmetrical (SUSY) transformation [25,26]. However, when extra bound states (number n) are eliminated, a SUSY transformation always introduces a repulsive core of centrifugal type, i.e., $v_s(r)\underset{r\to 0}{\sim}n(n+1)/r^2$, instead of the usual Yukawa-type core in local OBEP models. Furthermore, the invariance of phase shifts under a SUSY transformation holds only for a *given* partial wave.

Here, we want to consider the more general case of a repulsive core of intermediate strength. Furthermore, we want to preserve the invariance of the phase shifts in several not just in one partial waves. Most importantly, we do not want to introduce any superfluous bound states into our model from the very beginning. Therefore, we refrain from using the rigorous results of SUSY transformations and we look for a potential that is close to the phase-equivalent potential in the subspace $\mathcal{H}_Q$ orthogonal to a given bound state.

B. The Malfliet-Tjon potential

To be specific let us consider a particular example. As the initial potential we take the Malfliet-Tjon potential MT-V [41]. The MT-V potential is a simple scalar model for the *NN* interaction, which yields an average deuteron binding energy of -0.4136 MeV and describes the *average* $^3S_1$ and $^1S_0$ *NN*-phase shifts reasonably well up to energies of about 300 MeV:

$$V_{\text{MT-V}}(r)=g_R\frac{\exp(-\mu_R r)}{\mu_R r}+g_A\frac{\exp(-\mu_A r)}{\mu_A r}, \tag{30a}$$

where the parameters take the values

$$g_R=1458.05\ \text{MeV},\qquad g_A=-578.09\ \text{MeV},$$
$$\mu_R=3.11\ \text{fm},\qquad \mu_A=1.55\ \text{fm}. \tag{30b}$$

Next, we introduce an orthogonality condition to the function $\varphi_0(r)$ of Gaussian form:

$$\varphi_0(r)=N\exp\left(-\frac{r^2}{2r_0^2}\right). \tag{31}$$

This $(0s)$ harmonic oscillator (HO) function approximates quite well the projection of the six-quark bag $|s^6[6]\rangle$ onto the *NN* channel [13,23,27,39]. For various values of the HO radius r_0 we now determine the coupling constants g_R' and g_A' of the modified potential

$$V'(r)=g_R'\frac{\exp(-\mu_R r)}{\mu_R r}+g_A'\frac{\exp(-\mu_A r)}{\mu_A r} \tag{32}$$

TABLE I. The parameters of the modified potentials reproducing the *S*-wave phase shifts for the initial MT-V potential with different values of the ''projector radius'' r_0 and properties of the wave function.

r_0 [fm]	g'_R [MeV]	g'_A [MeV]	$r_{\rm node}$ [fm]	β (1 Mev)	χ^2(deg^2) per point	ϵ_0 [MeV]	$\tilde{\epsilon}$ [MeV]
0.00	1458.1	−578.1	0.00			−0.4136	
0.15	992.0	−511.0	0.25	0.03	0.40	−2.51	−0.385
0.18	673.8	−468.6	0.28	0.06	1.07	−7.55	−0.370
0.20	433.0	−438.0	0.30	0.07	1.70	−36.06	−0.364
0.25	−5.0	−389.0	0.35	0.16	2.50	−430.30	−0.399
0.30	−63.6	−403.0	0.40	0.28	1.60	−683.70	−0.611
0.40	−106.2	−494.0	0.50	0.47	0.05	−528.00	−0.919
0.50	−287.2	−582.5	0.60	0.63	0.10	−378.80	−0.880

acting in the subspace $\mathcal{H}_Q$, which ensure the best fit to the *S*-wave phase shift for the *initial* potential MT-V (30a), acting in the *full* space $\mathcal{H}$. For the sake of simplicity we do not change the inverse radii of the core, μ_R, and of the attractive potential μ_A.

The results of this fit for different values of radius r_0 are presented in Table I. It can be seen that a fit is possible for r_0 lying in the interval 0.15–0.5 fm. Thus, in the *subspace* $\mathcal{H}_Q$ orthogonal to $\varphi_0(r)$, the partial *S*-wave phase shifts for the potential $V'(r)$ of Eq. (32) reproduce fairly well the corresponding phase shifts of the initial potential (30a) in the energy range 0–300 MeV (see the χ^2 values in Table I). We do not present here the respective figures because the difference between the phase shifts of the initial potential MT-V and those of $V'(r)$ is almost indistinguishable in the graph.

It should be noted that the local core disappears already at $r_0=0.2$ fm. A further increase in r_0 results in an increase of the radius $r_{\rm node}$ of the internal node in the wave function and of the amplitude of internal loop specified by the ratio β of absolute values of the wave function in the first and in second maxima (see the fifth column in the Table I). After such a modification of the potential, the bound state energy ε_0 (*in the full space*) varies from -2.51 up to -600 MeV. However, if we require the orthogonality to φ_0, i.e., if we are operating *in the orthogonal subspace*, the bound-state energy $\tilde{\varepsilon}_0$ in Table I remains almost constant that is of the order of 1 MeV.

Thus, we obtain a series of approximately spectral-equivalent Hamiltonians.[2] The best (i.e., the smallest) value of χ^2 is obtained for $r_0=0.4$ fm when there are two bound states in the potential $V'(r)$: the first one is deep lying with the energy $\varepsilon_0=-528$ MeV (see the third row in Table I) and the second one is close to the *NN* threshold at the energy $\varepsilon_1=-0.4$ MeV, the eigenfunction of the deep bound state being very close to the HO function $\varphi_0(r)$. In other words, we arrive again at a deep attractive potential *without* any local repulsive core but with an eigenstate projector, that is, a construction very similar to the Moscow potential model. Thus, there are two extreme cases: (i) the deep purely attractive potential with the ''extra'' deep-lying state at $\varepsilon_0=-528$ MeV corresponding to $r_0=0.4$ fm, and (ii) the initial MT-V potential which does not contain the ''extra'' deep-lying bound state state at $\epsilon_0=-528$ MeV but has a local repulsive core instead.

These two phase shift equivalent potentials are approximate supersymmetric partners. All other cases in Table I can be considered as intermediate variants, lying between these extremes.[3] By changing the ''projector radius'' r_0 from zero to 0.4 fm, we perform a continuous transformation from one extreme model to the other. In doing so, the position $r_{\rm node}$ of internal node of wave function changes and the amplitude of the internal loop of the wave function increases. This can be seen in Fig. 1, which shows the scattering wave functions at 1 MeV for three potentials: the initial local MT-V (dashed line 1), the intermediate nonlocal potential with $r_0=0.2$ fm (solid curve 2) and the potential having an approximate eigenstate projector with $r_0=0.4$ fm (dotted curve 3).

We emphasize again that, the second extreme case with $r_0=0.4$ fm involves an almost exact eigenstate projector, i.e., for the given values of the coupling constants g'_R and g'_A (see Table I) the modified potential (32) leads to a deep-lying bound state with with energy $\varepsilon_0\simeq-528$ MeV. The corresponding eigenfunction is very close to $\varphi_0(r)$ at $r_0=0.4$ fm. Because the Hamiltonian is Hermitian, all scattering wave functions, and also the eigenfunction of the second (near-threshold) bound state at $\varepsilon_1=-0.41$ MeV are automatically orthogonal to the wave function of the deep-lying level. Hence, there is no need for any additional orthogonality conditions.

As a result, the supersymmetric partners are *local* potentials, while all phase-equivalent intermediate cases correspond to *nonlocal* interactions in the full space, or alternatively, to *local* interactions *in the subspace* $\mathcal{H}_Q$. However, according to our intention, we would like to obtain a good description not only in partial *S* waves, but also in *D* waves and possibly in other even partial waves. In a realistic hybrid model of the baryon-baryon interaction, a quark bag is formed only in the lowest partial waves. Therefore, the ad-

[2]In contrast to trivially spectral-equivalent Hamiltonians that are obtained as a result of the unitary transformation $H'=U^{-1}HU$ and which have been investigated in detail in the literature [42], our transformed potentials do not include any velocity dependence. Most importantly however, they have a different physical meaning.

[3]Such an intermediate model may be relevant for modelling the physical ω-meson exchange interaction with a reduced ωNN coupling strength.

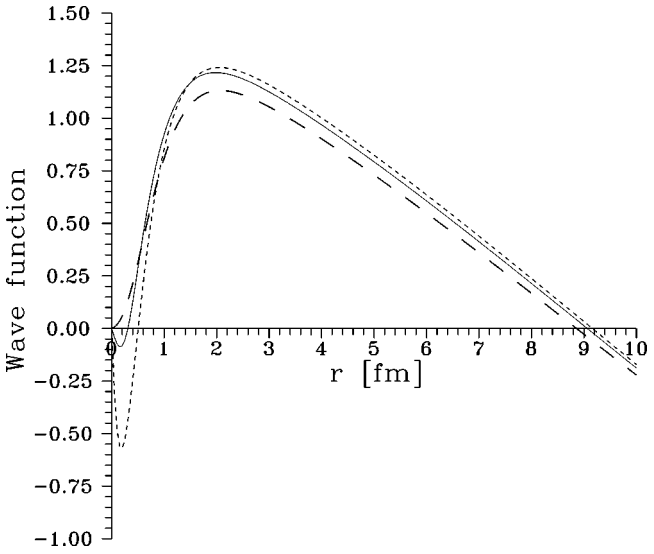

FIG. 1. The scattering wave functions at $E_{\rm lab}=1$ MeV for three S-wave phase shift equivalent potentials: initial local MT-V (curve 1), the intermediate nonlocal potential with $r_0=0.2$ fm (curve 2), and the purely attractive potential with the projector close to the eigenprojector with $r_0=0.4$ fm (curve 3).

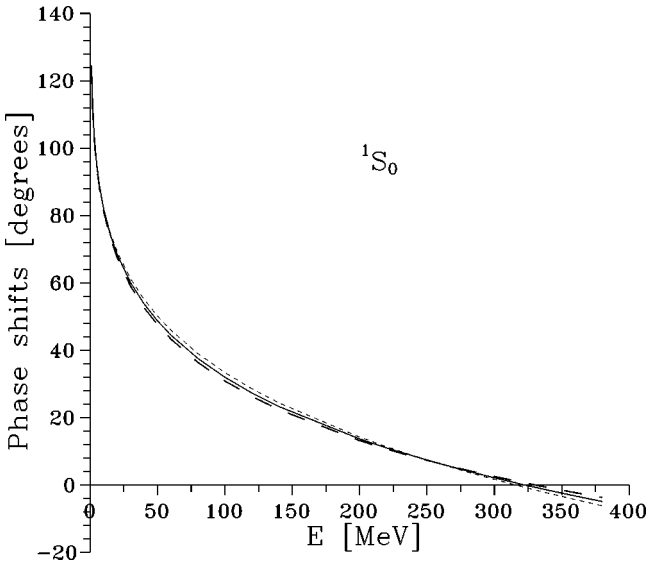

FIG. 2. *NN* S-wave phase shifts for center of mass energies between 0–400 MeV for the initial MT-V potential (dashed line) and for two modified potentials $V'(r)$ fitted to S- and D-wave phase shifts (see Table II): (i) with $r_0=0.15$ fm (solid line) and (ii) with $r_0=0.2475$ fm (dotted line).

ditional orthogonality condition must be included only in lowest partial waves (S and P), whereas *the same Hamiltonian* without any additional orthogonality constraints is expected to correctly describe the phase shifts in higher partial waves.

Thus, we attempt to find a modified potential (32) acting in the subspace $\mathcal{H}_Q$ that *simultaneously* describes the S- and D-wave phase shifts for the initial MT-V potential. This is possible with acceptable accuracy for various values of r_0. Table II presents several variants of the modified potential (32) with different values r_0 that are fitted to the S- and D-wave phase shifts under the condition that these are orthogonal to the S-wave function φ_0. Because we intend to use the above potentials in three-body calculations, we present here the versions for which the ''deuteron'' binding energies are practically identical ($\equiv 0.413$ MeV). The results of three-body calculations with these potentials are also given in the Table II and are discussed below.

Figures 2 and 3 show a comparison of the S- and D-wave phase shifts in the energy range 0–400 MeV for three potentials: (i) the initial local MT-V model, (ii) a modified nonlocal potential $V'(r)$ with $r_0=0.2475$ fm (i.e., a potential without a repulsive core that is close to the SUSY partner of the MT-V), and (iii) a modified nonlocal potential $V'(r)$ with $r_0=0.15$ fm (an intermediate variant). It is clearly seen that the potential with the strongly reduced repulsive core acting in the subspace $\mathcal{H}_Q$ provides a satisfactory description of both S- and D-wave phase shifts of the initial MT-V potential acting in the full space $\mathcal{H}$.

In this way, our simple toy model shows that the introduction of an additional condition which ensures orthogonality to some localized state φ_0 enables us to perform a *continuous transition* between the local core model and the model with ''extra'' bound states but no core. Both alternatives describe the interaction between composite nucleons equally well. The extreme models happen to be SUSY partners. In between, one has a series of almost phase shift

TABLE II. Variants of the MT-V potential with different values of the ''projector radius'' r_0, fitted to S- and D-wave phase shifts of the original MT-V potential and the two-body bound state energy $\varepsilon_0=-0.4136$ MeV, together with the corresponding results for the three-body calculations.

r_0 fm	g'_R MeV	g'_A MeV	E_3 MeV	T_3 MeV	%S	%D	$\approx E_3^{\rm rep}$ MeV	$q_{\rm min}$ fm^{-2}	$q_{\rm max}$ fm^{-2}	$F_{\rm max}$
MT-V	1458.05	−578.09	−8.25	30.6	99.0	0.75	−7.52	19	24.0	4.8×10^{-4}
0.15	999.36	−514.00	−8.42	40.3	98.5	1.1	−6.73	19	24.0	5.4×10^{-4}
0.18	800.00	−497.76	−8.45	44.3	98.0	1.3	−6.11	18	23.5	6.0×10^{-4}
0.20	445.80	−443.30	−8.82	51.8	97.8	1.7	−5.96	19	25.0	6.0×10^{-4}
0.25	0.00	−388.67	-8.99	74.6	97.0	2.0	−5.36	20	25.0	5.9×10^{-4}
0.30	−71.50	−394.50	−8.02	115.0	95.0	3.0	−4.20	21	27.0	4.0×10^{-4}
0.40	−69.87	−464.90	−7.02	189.0	89.0	5.8	−3.20	24	31.0	1.7×10^{-4}

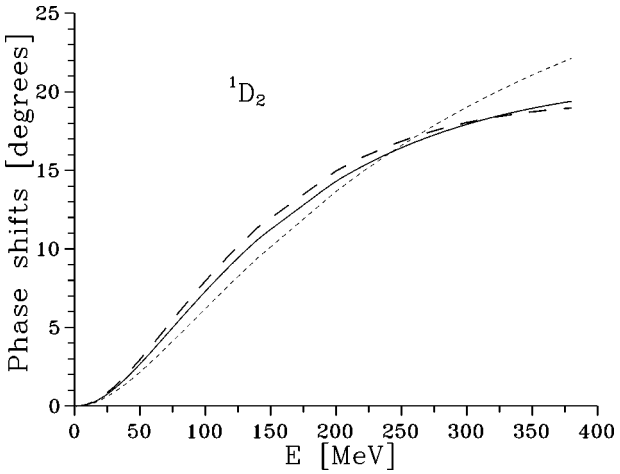

FIG. 3. *D*-wave phase shifts for the same three variants of the interaction potential as in Fig. 2.

equivalent potentials, differing by the core strength and by the spatial extension (r_0) of the state φ_0.

C. Consequences for three-nucleon bound states

Next we discuss, how the properties of the $3N$-system change when going from one NN-force model to the other. In Table II we compare the $3N$ predictions of the initial MT-V model Eqs. (30a) and (30b) with those of the different variants of the orthogonalized model. Table II displays bound-state energies E_3, kinetic energies T_3, and also the minimum and secondary maximum position of the ^{3}H charge form factor together with its value $F_{\max}$ in the secondary maximum for different variants of the potential (32) and different functions (i.e., different values of r_0) $\varphi_0(r)$.

One can see that an increase in the ''projector radius'' r_0 from 0 up to 0.25 fm leads to *an increase* of the three-body binding energy from 8.25 up to 8.99 MeV. As r_0 increases further up to 0.4 fm the binding energy begins to decrease again. These results contradict the results of Nakaichi-Maeda [43], who showed that the replacement of the local core by the orthogonality condition leads always to a *reduction* of the three-particle bound-state energy. According to [43], the ''stronger'' the imposed orthogonality condition, i.e., the larger the amplitude of the inner loop in the radial wave functions, the more pronounced the reduction of the binding energy. At first sight, our results seem to contradict the $3N$ calculations with the Moscow potential, undertaken by several groups (see, e.g., [44–46]). These calculations showed that the replacement of the local repulsive core NN potential (for example, the Reid potential) by the Moscow NN potential leads to a *reduction* of the binding energy from 7 down to 4.5 MeV [44].

The difference between our results and the Nakaichi-Maeda findings is explained as follows. The transition from the local core to the orthogonality condition causes a sharp increase in the kinetic energy of the $3N$ system (see the fifth column in Table II). This in turn leads to an increase of the contributions of higher partial waves. The main role is played by an attraction in D waves—see the seventh column in Table II. It should be emphasized that the MT-V potential is central and therefore does not mix three-body states with different values of the total angular momentum L. We consider here the mixing *within* a state of given total angular momentum L (e.g., $L=0$). By higher partial waves, we mean states with $\lambda = l = 2,4, \ldots$, where λ and l are angular momenta associated with the Jacobi coordinates r and ρ, respectively.

The change in the $3N$ binding energy thus depends on the magnitude and sign of the D-wave interaction: if this interaction is strongly attractive, the binding energy is increased, if it is repulsive the binding energy is decreased. To verify this statement, we have carried out $3N$ calculations with strong repulsion in D-wave interactions, while keeping the S-wave interaction fixed. The results are presented in the eighth column of Table II ($E_3^{\rm rep}$). With increasing r_0, i.e., with a strengthening of the orthogonality constraints, the contribution of the internal D wave grows and the binding energy $E_3^{\rm rep}$ with repulsive D-wave interaction monotonically decreases.

The calculations of Nakaichi-Maeda [43] and Hahn *et al.* [44] were based on the Faddeev equations and ignored the usually small contribution of higher partial waves. Under these restrictions, our calculation also shows that the orthogonality condition always leads to a stronger effective repulsion than the original local repulsive core model.[4] As a result, without the higher partial waves the binding of the $3N$ system becomes weaker as one goes from the local repulsive core model to an M-type model. If we include the contribution of higher partial waves in pair subsystems (for a fixed value of the total orbital angular momentum L), the $3N$ binding energy changes in the way described above. An appreciable increase of the contribution of the higher partial waves in pair subsystems due to the increase of the internal kinetic energy is the distinctive feature of M-type models. A more detailed discussion of this property is given below when we consider a more realistic model.

IV. THE MOSCOW POTENTIAL MODEL

A. One-channel model

Early attempts to construct an NN-potential with an additional ''forbidden'' state, i.e., a model of M type, were undertaken already in the middle of the 1970's [23]. However, in these early works only central potentials and only even partial waves were considered. We point out that these early attempts were undertaken yet *before* the color degree of freedom quark was fully established. But for colorless quarks (fermions), the lowest (as it then seemed) six-quark configuration $|(0s)^6[6]_X L=0,ST\rangle$ is strictly forbidden by the Pauli principle. Therefore, these NN potentials were interpreted in complete analogy with the effective potentials between nuclear clusters (e.g., the α-α potential), in other words, as potentials with bound states forbidden by the Pauli principle.

The first version of a realistic Moscow potential was suggested in 1983 [47] and further details can be found in Ref. [48]. This version describes the NN interaction only in the

[4]This is probably due to the fact that the radius of the separable repulsive core in the pseudo-potential $\mu|\varphi_0\rangle\langle\varphi_0|$ (for $\mu\to\infty$), is much greater than the radius of the original local repulsive core.

$^1S_0$ and $^3S_1$-$^3D_1$ channels. Later on the description was extended to the lowest odd parity partial waves ($^3P_0$, $^3P_1$, $^3P_2$-$^3F_2$) [49]. A new and improved version of the Moscow potential (version 86) was published in [50]. This version still had a node in the deuteron D wave for which there is no evidence in microscopic quark models [11,13,16]. Finally, in 1990, we have changed the truncation of the tensor OPE potential [27], which eliminated the D-wave node (version 90).

The main difference between the Moscow potential and standard models for the NN interaction is the absence of a local repulsive core at small distances. Instead of the core, the interaction is described by a deep attractive potential $V_0\exp(-\eta r^2)$ plus an appropriate condition of orthogonality to an extra deeply bound state. Owing to the deep-lying bound state, the physical NN wave functions have a node at small distances. The position of this node at around ~ 0.6 fm is almost stationary with increasing energy. In our approach, this stationary node plays the role of the repulsive core in standard models, and provides the correct behavior of the NN scattering phase shifts. The physical meaning of the ''extra'' bound states in the lowest partial waves has been repeatedly discussed in the literature [22,27,37]. They either simulate six-quark bag compound states, for example, $|s^6[6]_X\rangle$ in S waves, and $|s^5p[51]_X\rangle$ in relative P waves, which cannot be adequately described in terms of nucleon degrees of freedom only [13,15,17,22]; or they describe bound states in the nucleon plus Roper resonance $NN^*(1440)$ channel [37]. We recall that the interaction in the $NN^*(1440)$ channel must be very similar to the original NN interaction because the Roper resonance has the same quantum numbers as the nucleon.

Because we are mainly interested in the predictions of Moscow-type NN potentials for $3N$ systems, a more complete version of such potentials including even partial waves with $l \leqslant 4$ is necessary. Here, we present a few new versions for *even* partial waves. The form of the interaction for odd partial waves (for version 86) is discussed in [50]. An updated version of the Moscow potential for odd partial waves will be considered in a future publication. In accordance with general expectations, six-quark bags appear mainly in the lowest S and P partial waves (for $E_{\rm lab} \leqslant 800$ MeV). Therefore, the extra bound states describing the projections of these six-quark states onto the NN channel can occur only in these lowest partial waves.

In the higher partial waves there are no extra bound states and correspondingly no nodes in the wave function. However, an interaction that has in the lowest partial wave only an attractive local potential and a repulsive projector multiplied by a large positive constant, is too strong for higher partial waves. In order to take into account the short-range repulsion generated by ω-meson exchange, and in order to retain the universal form of the interaction in all partial waves, we add a repulsive core in the same separable form with a Gaussian form factor, as in the lowest partial waves, but with a *finite* positive coupling constant. We will then arrive at some *intermediate* model of the type discussed in the previous section.

The final Moscow potential consists of two parts. First, a local l-independent part, which explicitly includes the one-pion-exchange (OPE) potential and a deep attractive well $V_0\exp(-\eta r^2)$ that depends on the spin and parity of the NN system. Second, a state-dependent separable repulsive core with Gaussian form factor, which provides the correct D-wave phase shifts. This form of the potential is not only universal, but it is also convenient for three-body variational calculations, because it is possible to calculate all of the matrix elements of the Hamiltonian analytically [51–53]. The separable core providing the short-range repulsion depends on l and J. Therefore, it is not necessary to explicitly include a spin-orbit interaction for even partial waves.

The OPE potential is truncated in a suitable way at small distances (see below). The tensor interaction which couples partial waves with angular momenta l and $l \pm 2$ is in all partial waves quite reasonably described by the truncated OPE potential. Thus, the channel coupling is easily controlled by the truncation parameter. For partial waves with $l \geqslant 4$, the repulsive core is not required (for $E_{\rm lab} < 400$ MeV) since the phase shifts with $l \geqslant 4$ are completely determined by the long-range OPE tail of the interaction. Thus, the NN potential for even partial waves has the form

$$V_{NN} = V_{\rm loc} + V_{\rm sep}, \tag{33}$$

where $V_{\rm loc}$ is a local l-*independent* part of the interaction which, however, depends on spin and parity:

$$V_{\rm loc}(r) = V_C(r) + V_T(r)\hat{S}_{12}, \tag{34}$$

$$V_C(r) = V_0\exp(-\eta r^2) + V_C^{\rm OPE}(r) f_{\rm tr}(r), \tag{35}$$

$$V_T(r) = V_T^{\rm OPE}(r)[f_{\rm tr}(r)]^n, \tag{36}$$

where the cutoff factor is

$$f_{\rm tr}(r) = 1 - \exp(-\alpha r). \tag{37}$$

The exponent n is different for various versions of the model. The OPE potentials $V_C^{\rm OPE}$ and $V_T^{\rm OPE}$ have the standard form

$$V_C^{\rm OPE}(r) = V_0^{\rm OPE}\exp(-x)/x, \quad x = \mu r,$$

$$V_T^{\rm OPE}(r) = V_0^{\rm OPE}(1 + 3/x + 3/x^2)\exp(-x)/x.$$

We use an averaged π-meson mass μ and a πNN coupling constant $g_{\pi NN}^2/4\pi = 13.8$ [27,48,50]

$$V_0^{\rm OPE} = -\frac{g_{\pi NN}^2}{4\pi}\frac{\mu^3}{4M_N^2} = -10.69 \ \text{MeV}, \quad \mu = 0.6995 \ \text{fm}^{-1}.$$

The separable repulsive core $V_{\rm sep}$ has the form (for $l = 2$ and 3)

$$V_{\rm sep} = \lambda|\varphi\rangle\langle\varphi|, \tag{38}$$

$$\varphi = Nr^{l+1}\exp\left[-\frac{1}{2}\left(\frac{r}{r_0}\right)^2\right], \quad \int \varphi^2 dr = 1. \tag{39}$$

The strength constants λ for the separable core vary for different J and l, whereas the radius of the repulsive core r_0 varies only slightly from state to state (see Table III). For $l \geqslant 4$ the term $V_{\rm sep}$ is absent. Parameters for several variants of

TABLE III. Parameters of the Moscow *NN* potentials.

variant	parameter values				parameter values of r_0 [fm], λ [MeV] for particular channels					
	n	V_0 [MeV]	η [fm^{-2}]	α [fm^{-1}]	$^3S_1$		$^3D_2$		$^3D_3$	
	triplet channels									
A	3	−466.7	1.600	3.000	0.448	∞	0.4600	251.0	0.300	∞
B	3	−1329.0	2.296	1.884	0.445	∞	0.4061	427.2	0.276	∞
C	7	−1459.2	2.372	2.610	0.454	∞	0.4199	353.8	0.289	∞
	singlet channels				$^1S_0$		$^1D_2$			
a		−1106.2	1.600	3.000	0.4998	∞	0.4472	229.0		
b		−1220.0	1.753	1.884	0.4815	∞	0.4103	303.7		
c		−1222.0	1.738	1.000	0.4825	∞	0.4071	321.8		

the *NN* potential differing in the truncation of the tensor part in triplet-even channels are given in Table III. We have found (see Sec. IV) that the properties of *NN* and 3*N* systems calculated with M-type potentials (this is also true for conventional *NN* potentials [2,6–8,54] strongly depend on the behavior of the tensor potential at small distances). In the 1986 version of the Moscow potential [variant (A) in Table III], an exponential truncation of the tensor part [see Eq. (37)] with a value $n=3$ and an inverse radius of truncation $\alpha=3$ fm^{-1} was used. In that case, the tensor potential truncated according to Eqs. (36) and (37) corresponds to a large negative constant at the origin [$V_T(0)=-5500$ MeV]. Therefore, there is a very strong coupling of the $^3S_1$-$^3D_1$ channels at small distances. This coupling results in a large loop in the deuteron *D* wave, as well as in a large *D*-state admixture P_D of 6.4%. The relative amplitude of this loop $A^D_{\rm loop}$ compared to the maximum value of the *D*-wave function is given in Table III.

However, in view of the relatively weak quark-quark tensor force, it is desirable to have an interaction variant, for which the node in the deuteron *D* wave is absent. Such a variant was found in our previous work [27], where a step factor

$$f_{\rm tr}=\frac{(pr)^6}{1+(pr)^6}$$

has been used for the truncation. The steplike truncation leads, however, to technical difficulties when used in a three-body calculation. Therefore, we present here some alternative variants of the triplet-even potential which still have an exponential truncation factor $[1-\exp(-\alpha r)]^n$ with $n>3$, for which the relative magnitude of the *D*-wave loop varies from 0.5 down to 0.02. It is important to note that the stronger the truncation of the tensor potential, i.e., the weaker the tensor interaction at small distances, the larger the 3*N* binding energy (see the subsequent section).

The dependence of all observables on the truncation factor of the central part $V_C^{\rm OPE}$ is very weak. For example, a stronger truncation in $V_C^{\rm OPE}$ is easily compensated by a corresponding strengthening of the central attractive (Gaussian) part of the interaction. Therefore, in the present three-body calculations, we have used only one of the new variants for the singlet potential presented in Table III (namely, variant c). In addition, we have found that a fit to the experimental phase shifts in the interval 0–400 MeV does not uniquely determine the width η and depth V_0 of the deep potential in the central part of the *NN* interaction (35). Any variation of the width η can always be compensated by an appropriate variation of the depth V_0, without changing the quality of the phase shift fit. As a result, it is possible to choose the same width for the triplet $^3S_1$-$^3D_1$ (η_t) and the singlet $^1S_0$ (η_s) channels. Alternatively, it is possible to choose the same values of the depth V_0 in triplet and singlet channels. In this case the width η_s and η_t would be different.

We emphasize that the equality $\eta_s=\eta_t$ is impossible to reach in simple conventional potential models [1]. In other words, the width of the triplet potential is always different from that of the singlet potential. Both parameters (i.e., width and depth) of the conventional potential model are *uniquely* determined by the values of the low-energy effective range parameters, i.e., by the scattering length and effective range. It was recently found [55] that owing to some freedom in the choice of the three main parameters of the interaction, i.e., width η, depth V_0, and the truncation radius of the OPE potential α, the values of the width parameters η and α^2 can be taken to be equal, i.e., $\eta=\alpha^2$. We then obtain the simplest two-parameter model of the Moscow potential, where only two parameters (width and depth) are fitted to the scattering length and effective range of the $^1S_0$ partial wave. However,

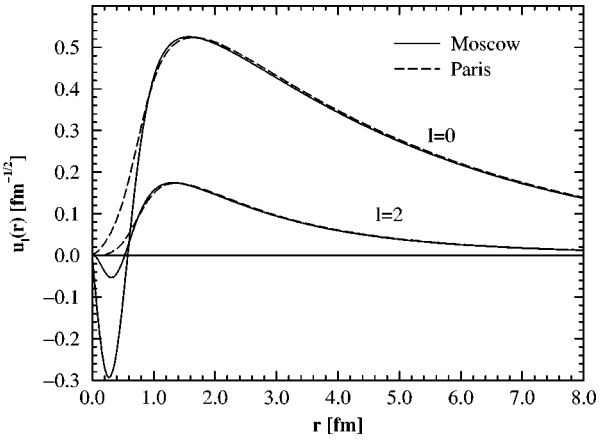

FIG. 4. The deuteron *S*-wave ($l=0$) and *D*-wave ($l=2$) functions for model B. The deuteron wave functions calculated with the Paris potential [5] are shown for comparison.

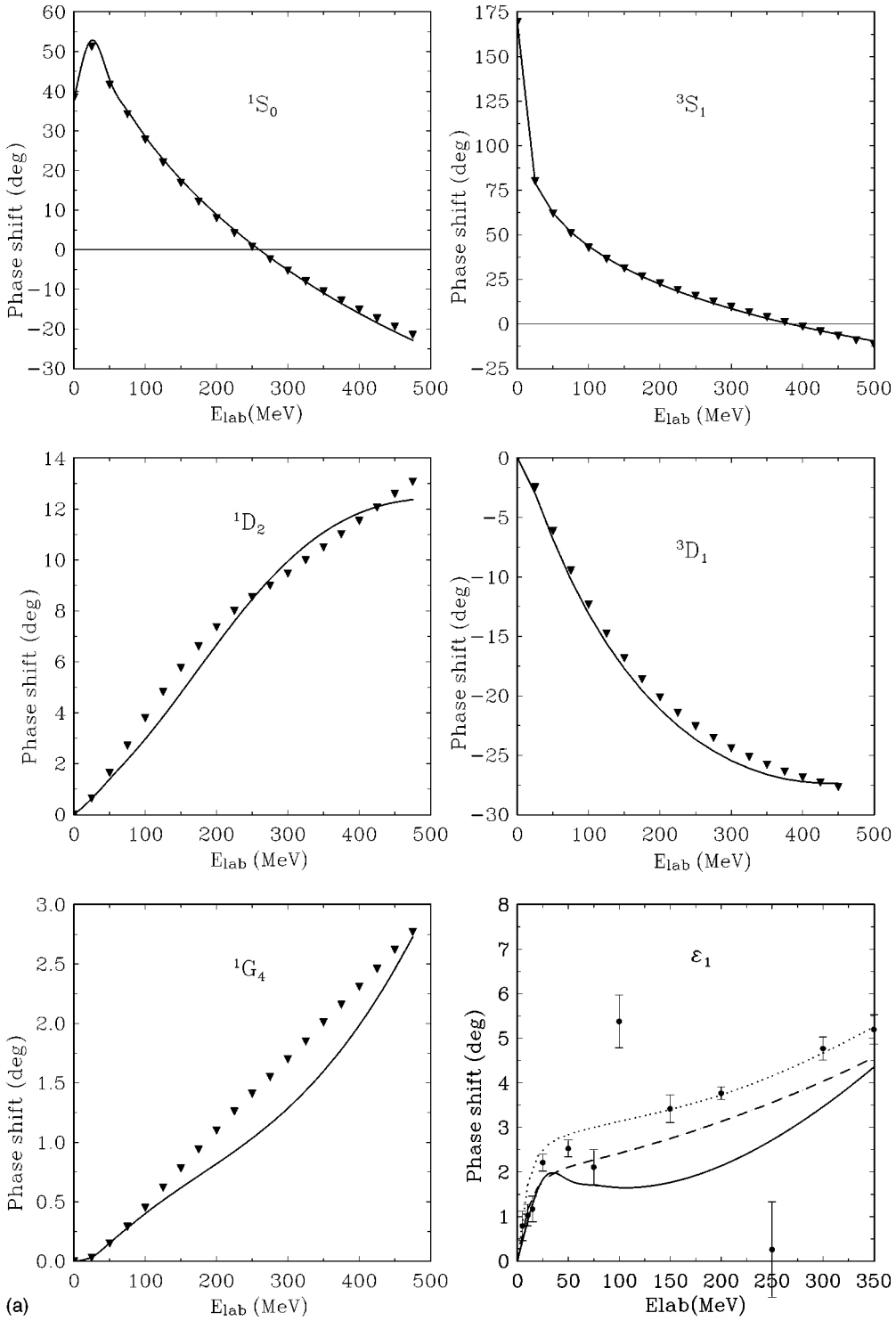

FIG. 5. The even parity phase shifts for the new version of the *NN* Moscow potential (variant B) are compared with the data of the energy-dependent phase-shift analysis by Arndt *et al.* [57] (triangles, dotted line for ε_1). For ε_1 we also show the Nijmegen phase-shift analysis PWA93 [58] (dashed line) and the single energy phase-shift analysis by Arndt *et al.* [57] (circles).

unlike conventional force models (see Ref. [1], Chap. 2), we obtain with this simplest two-parameter model an excellent description of the $^3S_1$-$^3D_1$ and $^1S_0$-wave phase shifts in a large interval of 0–500 MeV instead of a good fit only in the range between 0–15 MeV typical for conventional models. Simultaneously, we obtain a good description of the main static properties of the deuteron [55], including the quadrupole moment, charge rms radius and the asymptotic normalizations A_S and A_D.

We attribute this success to the choice of the proper degrees of freedom for a potential description. Conventional models try to describe both, the short-range six-quark and the long-distance one-boson exchange aspects of the *NN* interaction. This leads to a complicated energy and momentum dependence of the resulting *NN* potential. We claim that the Moscow potential model is so simple, because we do not try to cast the six-quark aspects of the *NN* interaction into the same formalism as the asymptotic long-range part. The six-

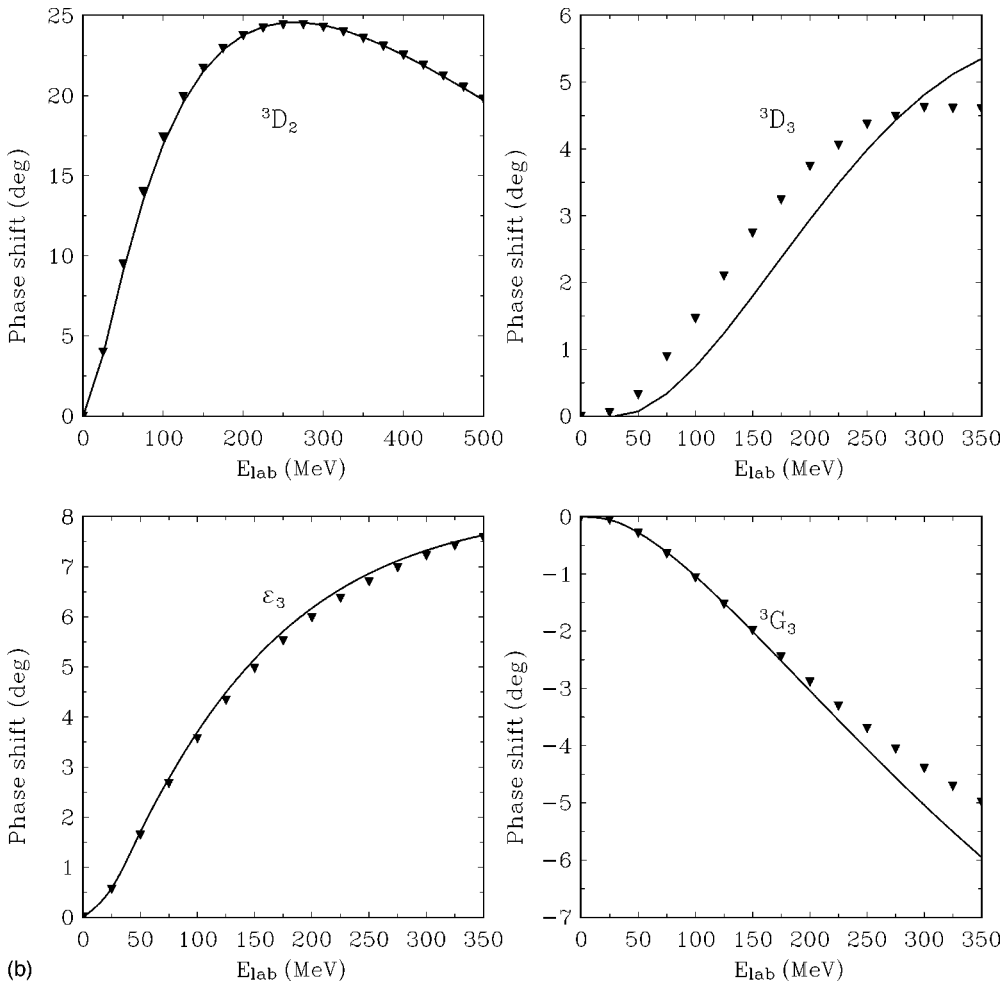

FIG. 5. (*Continued.*)

quark aspects in the *NN* sector are more adequately described by an orthogonality condition, rather than by a local repulsive *NN* potential.

The parameters of the Moscow potential model are listed in Table III. The deuteron wave function calculated with model B is shown in Fig. 4. In Fig. 5, the phase shifts of the *even* partial waves for variant (B) are compared with the experimental ones [57]. The description of the *NN* phase shifts is for all variants listed in Table III quite reasonable. However, our description of the mixing parameter ϵ_1 especially for energies $E>400$ MeV, is not yet satisfactory. The mixing parameter ϵ_1 is determined by the value of the matrix element $\langle\Psi_S|V_T|\Psi_D\rangle$. Our overestimation of ϵ_1 at higher energies is a consequence of the behavior of the $^3S_1$ and $^3D_1$ eigenfunctions at short distances. While the *S* wave has a node and a rather pronounced loop, there is almost no loop in the *D* wave. This leads to a rather sharp increase of ϵ_1 at higher energies.[5] In the more complete two-channel model, the short-range *S*-wave loop should be significantly reduced and we expect a flatter behavior of ϵ_1 in better agreement with modern data.

[5]In contrast to this, in the first version of the Moscow potential model [48], there were two coinciding nodes and loops in both the *S* and *D* waves and a rather satisfactory fit to ϵ_1 was obtained.

B. Exclusion of the deep-lying bound state

The ''extra'' bound states in *S* and *P* waves have to be excluded if the potential is used in few-nucleon calculations. As was already discussed in Sec. II, this is most conveniently done by means of the orthogonalizing pseudopotential (OPP):

$$V_{\rm OPP}=\lambda\Gamma, \quad \Gamma=|\varphi_f\rangle\langle\varphi_f| \tag{40}$$

with a large positive value of the strength constant λ [24,59]. In practice a value of $\lambda\sim10^5-10^6$ MeV is quite sufficient. In the case of coupled channels $^3S_1$-$^3D_1$ and $^3P_2$-$^3F_2$ the function φ_f in Eq. (40) has two components. Therefore, it is necessary to use a two-channel *matrix* projector of the form

$$\hat\Gamma_2=\begin{pmatrix}|\varphi_f^1\rangle\langle\varphi_f^1| & |\varphi_f^1\rangle\langle\varphi_f^2|\\ |\varphi_f^2\rangle\langle\varphi_f^1| & |\varphi_f^2\rangle\langle\varphi_f^2|\end{pmatrix}, \tag{41}$$

where $|\varphi_f^1\rangle$ and $|\varphi_f^2\rangle$ are the upper and lower entries of a two-component column vector, corresponding to the ''extra'' bound state. However, the matrix projector considerably complicates three-body calculations. Therefore, we use instead a one-component projector:

$$\hat\Gamma_2\to\hat\Gamma_1=\begin{pmatrix}|\tilde\varphi_f\rangle\langle\tilde\varphi_f| & 0\\ 0 & 0\end{pmatrix} \tag{42}$$

acting on the ''main'' channel, i.e., on the channel possessing highest weight in the ''extra'' state. In other words, in $^3S_1$-$^3D_1$ channels we use only an S-wave projector. In this case the function $\widetilde{\varphi}_f$ is selected so that the inclusion of the above one-component projector into the Hamiltonian gives a result that is as close as possible to the action of the *two-component* eigenprojector Γ_2. Strictly speaking, the replacement of the matrix projector (41) by a single-channel projector (42) should cause some modification of the appropriate NN phase shifts. We have found, however, that this replacement influences the description of the phase shifts in coupled channels only very weakly. Moreover, employment of the simple Gaussian function with suitable values of r_0 in $\widetilde{\varphi}_f$ can ensure a quite reasonable and accurate description of scattering phase shifts.

We will show, in particular, how the approximate S-wave projector $\Gamma=|\widetilde{\varphi}_f\rangle\langle\widetilde{\varphi}_f|$ acts in the coupled $^3S_1$-$^3D_1$ channels. The dependence of the first two energy levels on the orthogonalizing coupling constant λ for the $^3S_1$-$^3D_1$ channels is shown in Figs. 6(a) and 6(b) for the potential (B). If the projector is absent, there are two bound states: the ''extra'' ground state with energy $E_0=-599$ MeV with a D-wave probability of 6.3%, and the second bound state describing the physical deuteron with $E_1=-2.2245$ MeV and a D-wave probability of $P_D=5.75\%$. If the exact two-component state φ_0 is used in Γ_1, the energy of the ground state E_0 is shifted by an amount λ when λ is varied, whereas the deuteron energy E_1 does not vary at all (by definition). The deviation of the curves $E_0(\lambda)$ and $E_1(\lambda)$ from the straight line characterizes the difference between the application of the approximate (single-channel) S-wave projector and the exact matrix eigenprojector $\hat{\Gamma}_2$. As one can see, this difference is only important in the narrow range of values $\lambda=685-690$ MeV, where the energies E_0 and E_1 of both states come close to each other and the states are mixed strongly due to approximate orthogonality of $\widetilde{\varphi}_f$ and φ_1 (their overlap being $\langle\widetilde{\varphi}_f|\varphi_1\rangle=0.001$). For $\lambda>690$ MeV, the deuteron state becomes the new ground state and its energy grows very slowly with λ approaching the limiting value $E(\infty)=-2.2246$ MeV. On the other hand, the original ground state energy $E_0(\lambda)$ continues to rise and finally transforms into a narrow resonance. In the case of the exact eigenprojector, it would be transformed into a bound state embedded into the continuum with the positive energy $E_0+\lambda$. This resonance strongly distorts the phase shifts only in a narrow energy range near $E_{\text{c.m.}}=E_0+\lambda$. But since the values for λ used in the present three-nucleon calculation are of the order of $\lambda\sim10^6$ MeV, this distortion is far away from the physically relevant region. It is worth to note that if one takes only the S component of the *exact* wave function φ_0 as $\widetilde{\varphi}_f$ in the single-channel projector (42), the result turns out to be much worse. In other words, the result of the application of the projector $|\varphi_0^{(1)}\rangle\langle\varphi_0^{(1)}|$, i.e., *using the exact* first component of two-component vector, differs much more from the matrix eigenprojector $\hat{\Gamma}_2$, than the *approximate* projector $|\widetilde{\varphi}_f\rangle\langle\widetilde{\varphi}_f|$. This is explained by the fact that the orthogonality condition which is automatically satisfied for the eigenprojector $\hat{\Gamma}_2$ is

$$\langle\Phi_0|\Phi_1\rangle=\langle\varphi_0^{(1)}|\varphi_1^{(1)}\rangle+\langle\varphi_0^{(2)}|\varphi_1^{(2)}\rangle=0. \tag{43}$$

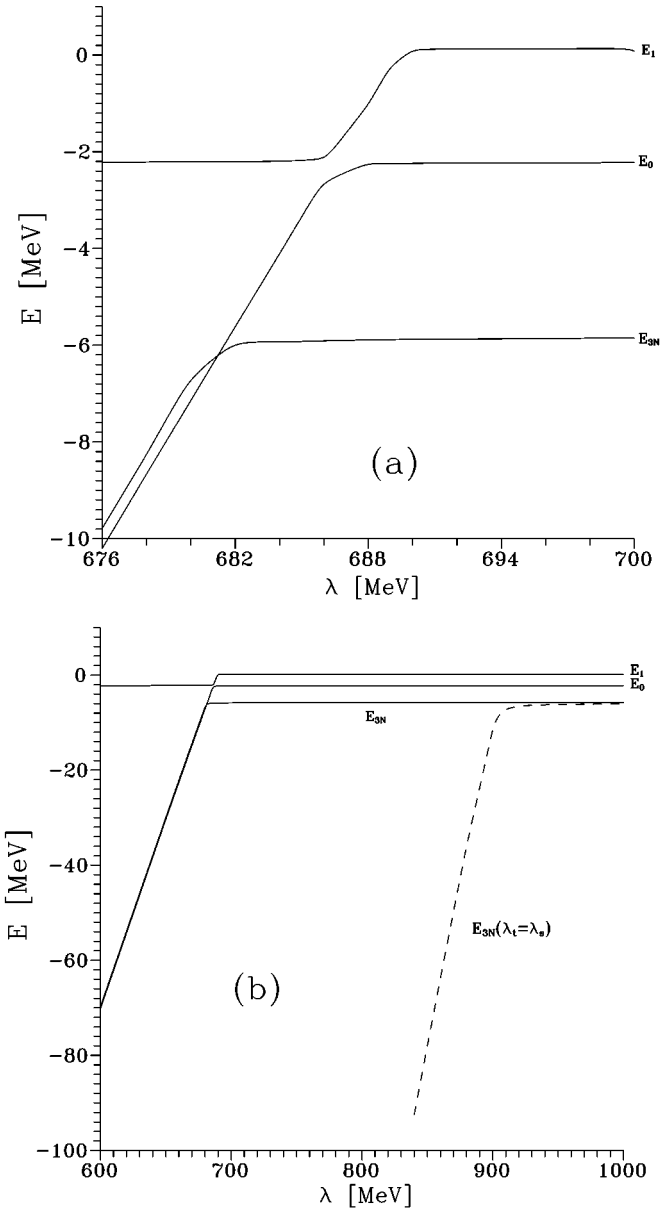

FIG. 6. (a) Effect of the approximate S-wave projector on the discrete spectra of $2N$ and $3N$ systems. E_0 and E_1 are the energies of the first two $2N$ states, E_{3N} is the energy of $3N$ ground state, λ is the $^3S_1$-wave projector coupling constant. (b) The dotted line shows the dependence of the $3N$-bound state on λ for the case $\lambda_s=\lambda_t$.

From here it does not follow, in general, that $\langle\varphi_0^{(1)}|\varphi_1^{(1)}\rangle=0$. At the same time it is possible to make the overlap of the deuteron with some approximate function $\widetilde{\varphi}_f$ arbitrarily small. Then the energy E_1 will not depend on λ, as in the case of the application of the exact eigenprojector $\hat{\Gamma}_2$. However, it is impossible to choose a simple approximate function that will be orthogonal to the scattering wave functions of the continuous spectrum for *all* energies. Therefore, due to the employment of the approximate projector, the scattering phase shifts are inevitably distorted in some small energy interval.

Bearing in mind the use of the potential in the three-nucleon system, where large values of the constant λ are needed, we restrict ourselves to the approximate projector

TABLE IV. Deuteron predictions for the different versions of the triplet-even Moscow *NN* potentials. $D_{\rm loop}$ is the amplitude of the *D*-wave loop. The deuteron matter radius is defined as $r_m^2 = 1/4 \int_0^\infty dr r^2 [u^2(r) + w^2(r)]$. For the most recent value of the deuteron matter radius see Ref. [56]. Here, η is the asymptotic D/S ratio. In impulse approximation (model B) the deuteron magnetic moment is $\mu_d = 0.847\ \mu_N$, the quadrupole moment is $Q_d = 0.271$ fm^2, and the charge radius is $r_{ch} = 2.112$ fm.

Variant	χ^2	$D_{\rm loop}$	E_d [MeV]	P_D%	η	r_m [fm]
A	118	0.50	−2.2244	6.59	0.0267	1.96
B	56	0.30	−2.2246	5.75	0.0258	1.95
C	126	0.02	−2.2246	6.14	0.0262	1.94

with a simple Gaussian form factor. Then the additional pseudopotential $V_{\rm sep}$ has the form of Eq. (40) in all channels. For *S*- and *P*-partial waves, the constants λ have to be sufficiently large ($\sim 10^5 - 10^6$ MeV) in order to ensure the exclusion of ''extra'' bound states, while their values in *D* waves are determined by fitting the experimental phase shifts. The corresponding values of r_0 for the approximate projector are also given in Table III. In the $^3D_1$ channel and in all higher partial waves with $l > 3$, the term $V_{\rm sep}$ is absent.

V. PROPERTIES OF THE THREE-NUCLEON BOUND STATE

Here, we discuss the predictions of the new versions of the Moscow model described in Sec. IV. The $3N$ calculations have been done by a variational method on a very large, nonminimal and nonorthogonal Gaussian basis [52,60] and are, in general, rather similar to the very accurate $3N$ calculations of Kameyama *et al.* [53]. With this basis the *absolute* accuracy for the eigenenergy is about 100 keV. The *relative* accuracy for the Coulomb displacement energy is even higher.

As follows from many previous $3N$ bound state calculations, the total contribution of odd partial wave interactions to the $3N$ binding energy is small and does not exceed 0.2 MeV [3]. We emphasize that odd partial waves have been included in our variational basis for the $3N$ bound state calculation but we did not take into account the contribution of the odd partial waves in the *NN* force. In the *NN* force, we include all *even* partial waves up to total orbital angular momentum $L = 4$. Our results are presented in Table V, where we list several static properties of ^{3}H and ^{3}He such as binding energies E, root-mean-square charge radius $r_{\rm ch}$, the percentages of D (P_D) and P waves (P_P), and the Coulomb displacement energy $\Delta_{\rm Coul}$ for the difference $E_B(^3{\rm H}) - E_B(^3{\rm He})$. In addition, we list the average kinetic energy T in the ground state, as well as certain characteristics of the ^{3}H charge form factor, i.e., the position of the first minimum $q_{\rm min}$, the second maximum $q_{\rm max}$ and the value of $|F_{\rm ch}|$ in the second maximum $F_{\rm max}$.

A. Dependence on the projection constants

First, we discuss the dependence of the three-nucleon properties found with the above force model on the projection constants λ. In Figs. 6(a) and 6(b) we show the dependence of the $3N$ ground state energy E_{3N} on the value $\lambda(^3S_1)$ multiplying the projector Γ, projecting onto an ''extra'' bound state in the $^3S_1$ channel. The two-body state energies $E_0(\lambda)$ and $E_1(\lambda)$ shown in Fig. 6 were already discussed in Sec. IV. All other parameters of the potentials are fixed, including the constants λ for the other channels. For $\lambda < 680$ MeV the $3N$ system remains unbound and the variational value E_{3N} practically coincides with the energy of the two-body ground state E_0. When λ is increased beyond 682 MeV, the system becomes bound with $E_{3N} = -6$ MeV. If λ is increased further the three-nucleon binding energy decreases very slowly approaching its limiting value $E_{3N}(\infty) = -5.74$ MeV, because these test calculations were done in a comparatively small basis. The saturation occurs for $\lambda = 10^5 - 10^6$ MeV. For higher values of λ the numerical results become unstable. The convergence of variational calculations with respect to λ was investigated in some detail in Ref. [61]. The physical deuteron becomes the ground state of the two-nucleon subsystem for $\lambda > 688$ MeV when $|E_{3N}|$ is already less than 6 MeV.

These results clearly show that it is impossible to fit the binding energy of the three-body system to the experimental value by adjusting the parameter λ. It is interesting to note that the system becomes bound when the repulsion in pair subsystems increases.[6] The reason of this interesting phenomenon is the following. When the projection constant in the singlet channel is chosen as, e.g., $\lambda_s = 10^6$ MeV and the one in the triplet channels as, e.g., $\lambda_t \ll 10^6$ MeV (and varying), the almost complete space symmetry of the three-nucleon system is broken, and the weight of wave function components with mixed orbital permutational symmetry $[21]_X$ is increased.

On the other hand, if the constants $\lambda(^3S_1)$ and $\lambda(^1S_0)$ evolve simultaneously, we find a different behavior $\widetilde{E}_{3N}(\lambda)$ that is shown by the dashed line in Fig. 6(b). Now, the $3N$ system remains bound for all λ. However, for the allowed values of λ that is when both ''extra'' bound states in the triplet and singlet channels are pushed sufficiently high above the physical state, the three-nucleon binding energy $|E_{3N}|$ appears at a value less than 7 MeV. So, in this case it is also impossible to fit the three-nucleon binding energy by shifting the ''extra'' two-body state to the positive energy region. Therefore, all results for the three-nucleon system discussed below have been calculated with sufficiently large values λ_s and $\lambda_t (\sim 10^5 - 10^6$ MeV) for which complete saturation has been reached, and the results are, in some sense, λ independent.

B. Binding energy of ^{3}H and ^{3}He

All variants of the model studied here differ only in the form of the truncation factor for the OPEP-tensor force at small distances and lead to overall similar results (see Tables III–V) except for one previous version of our model [50] (variant A in Tables III–V). In the course of the calculations we have found that the stronger the cutoff in OPEP tensor

[6]Certainly, the absolute value of three-body binding energy decreases in the process, however, the energy of the two-body threshold decreases still more quickly.

TABLE V. Three-nucleon properties with the A, B, and C versions of the Moscow potential.

variant of potential	$E(^3H)$ MeV	$T(^3H)$ MeV	P_D %	P_P %	$r_{ch}(^3H)$ fm	Δ_{Coul} MeV	$r_{ch}(^3He)$ fm	q^2_{min} fm^{-2}	q^2_{max} fm^{-2}	$F_{ch}(^3H)_{max}$
A	−5.07	143.7	7.8	0.03	2.15	0.612	2.41	13	18	1.2×10^{-3}
B	−6.03	162.4	7.4	0.03	2.01	0.670	2.24	16	22	9.6×10^{-4}
C	−6.03	162.8	8.1	0.05	2.01	0.667	2.25	16	22	9.6×10^{-4}
extrapol. to E_{exp}	−8.48	175.1	8.5	0.06	1.88	0.737	2.07	17	23	1.0×10^{-3}
experiment	−8.48				1.76	0.764	1.96	13	18	4×10^{-3}

force, the larger the $3N$ binding energy (see Tables III–V). In this respect our results are very similar to those found by Sasakawa and Ishikawa [54]. In their $3N$ studies with the Reid-soft-core (RSC) NN potential using various truncation factors of the tensor force they found that when the tensor force is cut off more strongly at short distances (and the central attractive part is correspondingly increased in order to keep the deuteron binding energy invariant), the $3N$ binding *rises* as well.

However, there is an important difference between the present results and those in Ref. [54]. In our case, the partial replacement of the short-range tensor force by a central force does not lead to a noticeable reduction of the tensor mixing parameter ε_1. In fact as the truncation is increased, the mixing parameter does not tend to zero, but, instead of this, it rises more sharply for larger n. This is related to the essentially different character of interference between tensor and central force (both in $2N$ and $3N$ systems) in our case as compared to the traditional nuclear force models (see the last paragraph in Sec. IV A). However, we do not expect drastic effects of our ϵ_1 description on the $3N$ binding energy, at least not within the corridor given by the different versions of our model. In fact, the difference in ϵ_1 values between the RSC and the Paris potential model is of the same size as that between the present version and experiment [62].

The ^{3}H binding energies obtained in the present study ($\sim$6.05 MeV) for the two most realistic variants of the potential (B and C) are much higher than the value of $\sim$4.5 MeV obtained by Hahn *et al.* [44] in their first $3N$ calculation with the earlier version of the Moscow potential. This large difference is caused by the following reasons.

(i) In the Hahn *et al.* [44] calculation and also in the early 1983 version of the Moscow potential an old version of the singlet $^1S_0$ potential fitted to the 1983 phase shift analysis [63] was employed. Our new singlet potential is fitted to the SAID database of 1995 [57] and resulted in some increased $3N$ binding (about $\sim$0.2 MeV).

(ii) Another, more important reason for the present improvement of the $3N$ results is the use of a stronger truncation of the short-range OPEP tensor force and the respective reduction of P_D in the deuteron and $3N$ systems—see the versions B, C, and D in Table IV. The sharper truncation removes or suppresses to a significant degree the inner node and the respective loop in the D wave at short distances.

(iii) A very restricted configuration space of only five basic channels $^3S_1$-$^3D_1$ and $^1S_0$ was employed in the Faddeev calculation of Hahn *et al.* [44] and the contribution of all $l>2$ higher partial waves was neglected. The latter contributions are quite important in our case especially in the Faddeev-like $3N$ approach.

We have previously emphasized the extremely important contribution of higher partial waves as manifested by a sharp increase of the average $3N$ kinetic energy. Compare the third column in Table V with the corresponding results [10,64] for traditional force models, in particular for model B:

$$E^{3N}_{kin}(\text{Paris})=42.6\ \text{MeV}, \quad E^{3N}_{kin}(\text{RSC})=49.3\ \text{MeV},$$

while

$$E^{3N}_{kin}(\text{Moscow})\simeq 150\ \text{MeV}$$

is more than three times higher. It is worth to recall here that the modest 20% increase in the average kinetic energy in the RSC potential as compared with the Paris potential, results already in an enhancement of the contribution of higher partial waves to the binding energy by as much as a factor of 2.5. Thus, one can easily imagine how large a contribution from higher partial waves may result in our case. A more detailed analysis of these results will be carried out elsewhere.

We must keep in mind that, contrary to conventional force models, our NN potential corresponds only to a one-channel approximation of the complete two-phase model, that is by the definition of the NN potential, only the effective NN channel with unexcited nucleons. As was argued above, the effective channel potential is phase-shift equivalent to the initial two-phase interaction model of hybrid type [see Eqs. (19) and (24)] and the replacement of the local repulsive core by a two-channel interaction model (e.g., as in case of QCB model by Simonov [15]) will lead to some additional binding of the order of some $\sim$0.8–0.9 MeV [65], simply because of the *presence* of the second channel. There is an additional reason for extra-binding in $3N$ and generally in many-nucleon systems if the full two-phase interaction model is considered. One has to take into account the interaction between the six-quark bag and the spectator nucleon. This dynamical $6q$-N channel coupling can be considered as some kind of three-body force that will also increase the $3N$-binding energy. We expect that these effects will mainly change the *absolute* values of the energies while the *relative* energies, which will be discussed in the following, will be

influenced only weakly. This is because the weights of the 6 q-bag components in ^{3}H and ^{3}He are small and have almost equal magnititude.

C. Coulomb displacement energy, charge radii, and form factors

As follows from the results displayed in Table V, the Coulomb displacement energy

$$\Delta_{\rm Coul} = E_B(^3{\rm H}) - E_B(^3{\rm He})$$

(for variants B and C with $n=5$ and 7 for the OPEP tensor force truncation) equals

$$\Delta_{\rm Coul} \simeq 670 \ \ {\rm keV}$$

for $E_B(^3H) = 6.05$ MeV. For a more careful test of the model, it is important, however, to find the value of $\Delta_{\rm Coul}$ when $E_B(^3H)$ is scaled to its experimental value -8.48 MeV since the larger the $3N$ binding energy the smaller the rms charge radius and the higher the Coulomb energy of ^{3}He. Thus, we slightly increase (by $\sim 2\%$) the strength of the central (triplet and singlet) potential well to fit the experimental value of $E_B(^3H)$, and for this case we analyze the Coulomb energy of ^{3}He and the rms charge radii of ^{3}H and ^{3}He with our model (see the two last rows in Table V).

The extrapolated Coulomb displacement energy turns out to be

$$\Delta^{\rm extra}_{\rm Coul} = 737 \ \ {\rm keV}$$

which is only 27 keV less than the experimental value. Here, we note in passing that in the full two-phase model calculation the magnitude of $\Delta_{\rm Coul}$ would increase further because the second channel comprises the more tightly packed $6q+N$ configuration.

The most likely reason for this improvement in the prediction of $\Delta^{\rm extra}_{\rm Coul}$ is the appearance of the inner radial nodes and corresponding short-range loops along every interparticle r_{ij} coordinate (and also along both Jacobi coordinates) in our $3N$ wave functions. The inner loops along the r_{ij} coordinates have only a minor influence on the rms radii of the charge or matter distribution because the latter are determined mainly by *one-particle* coordinates r_i (as measured from the center of mass). Contrary to this, the Coulomb potential between two protons in ^{3}He is maximal just at zero interparticle separation r_{ij} where we have some enhancement of particle density due to the presence of the inner loops in our wave functions.

This naturally explains why conventional force models leading to a short-range suppression of the wave functions along every interparticle distance miss some 100 keV in the Coulomb energy of ^{3}He, whereas our model, due to the inner loops leads to a prediction that is close to the experimental value. Although our result is still qualitative in the sense that it involves an extrapolation to the empirical binding energy, the observation that the inner wave function loops are extremely important for the Coulomb displacement energy is likely to survive. Moreover, if the force model presented here is corroborated in subsequent studies, it would suggest that inner loops are ubiquitous in nuclear wave functions.

The recent quantitative explanation of the Coulomb displacement energy in the literature [66] using a force model with a repulsive core is based on the assumption of a rather strong charge symmetry breaking (CSB) term $V_{\rm CSB}$ (difference between the np and nn strong interactions). With $V_{\rm CSB}$ added to the Argonne V_{18} potential, one can almost completely explain the 100 keV difference in $\Delta_{\rm Coul}$ between ^{3}He and ^{3}H. However, the same $V_{\rm CSB}$ leads to a strong overestimation of the Coulomb energy difference in the ^{6}Be-^{6}He system. Therefore, it is conceivable that the contribution of the charge symmetry breaking term $V_{\rm CSB}$ in Ref. [66] is actually smaller. In any case, it is evident from the discussion above that the assumption of a strong charge symmmetry breaking interaction $V_{\rm CSB}$ is not the only mechanism that can explain the 100 keV Coulomb energy difference in the $3N$ system.

The values of the extrapolated charge radii of ^{3}H and ^{3}He (see last row in Table V) turn out to be larger than the corresponding experimental values. However, it should be emphasized once again that the $3N$ calculations with the one-component force model presented here, i.e., carried out only in the NN (or $3N$) sector, corresponds just to the projection of the total two-phase model wave function onto the pure $3N$ component. The two-phase solution includes also compact $6q+N$ components with a sizeable probability, which may considerably reduce the $3N$ charge radius. Similarly, the full two-phase model will lead to important modifications in the charge form factors of ^{3}H and ^{3}He. Our results for the ^{3}H charge form factors calculated with the one-phase Moscow

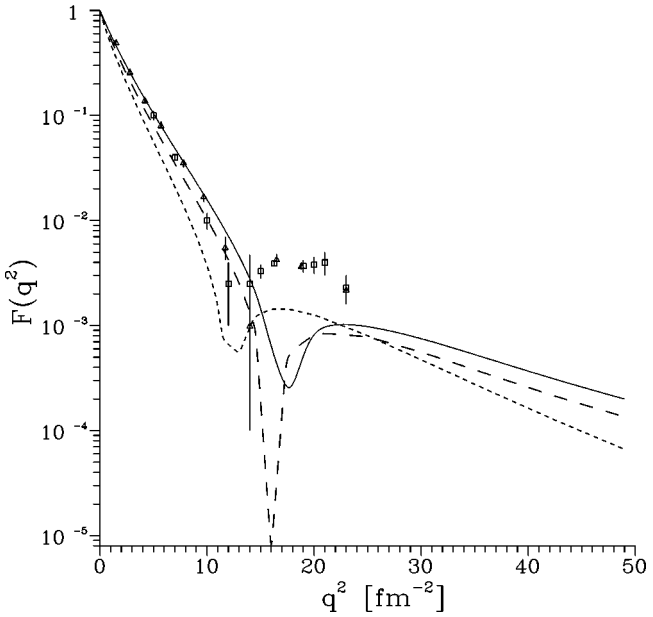

FIG. 7. The charge form factor of ^{3}H for different versions of the Moscow NN potential: the previous version (A) (short-dashed line), the present version (variant B) (dashed line), and the potential extrapolated to $E_{\rm exp}(^3{\rm H})$ (solid line). Also shown are the previous ($\Box$) and the new [68] ($\triangle$) experimental data.

potential are displayed in Fig. 7 together with the predictions for the extrapolated [to experimental $E_B(^3H)$] solution. We see that the behavior of the form factor for $q^2>14$ fm^{-2} is rather similar to predictions calculated with a conventional force model such as the RSC potential. However, we expect appreciable modifications for $q^2>14$ fm^{-2} for the original two-phase model, in which the sign of the $6q+N$ component is *opposite* to that of the main $3N$ component [13]. According to Refs. [65,67] this fact should considerably improve the description of the $3N$ charge form factors in the secondary maximum.

Summarizing we conclude that the description of both the $3N$ binding energy and some important $3N$ observables will presumably improve when passing from a one-phase potential model to a two-phase model due to the explicit appearance of the $6q+N$ component in the three-body solution.

VI. CONCLUSION

The force model presented in this paper—referred to as the M-type model–differs in a few important aspects from traditional NN interaction models currently in use.

First, M-type models necessarily incorporate additional orthogonality condition(s) with respect to certain nodeless functions φ_0. The orthogonality condition can be interpreted as the projection of six-quark compound states φ_0 with maximal space (or permutational) symmetry onto the asymptotic NN channel.

Second, M-type models are characterized by the presence of a deep attractive well while a part of the short-range repulsive core (or the whole core) is replaced by appropriate orthogonality conditions.[7] The consequences of the different off-shell behavior of conventional and M-type NN force models can be tested using NN bremsstrahlung [69].

Finally, the models presented here have a physical interpretation that is rather different from that of conventional force models. A standard force model aims at describing the NN interaction in the total configuration space in the form of some potential. Contrary to this, we start from the assumption that certain six-quark compound states of maximal permutational symmetry are present in the lowest partial waves. The latter have only very small projections onto the nonantisymmetrized asymptotic NN channel. However, at the same time they are strongly coupled by the six-quark Hamiltonian with the clusterized NN channel at small distances $r<1$ fm. As a result, these compound states cannot be described by *any* reasonable NN potential. These states can only be described by a very complicated nonlocal and energy-dependent NN interaction operator. However, even when utilizing such complicated interaction operators [70] we are forced to introduce many adjustable or free parameters to fit the data. Thus, due to the formation of the above compound six-quark states, the whole system cannot be described by any simple NN potential. In order to get an efficient potential description, it is necessary to remove the above *nonpotential pieces* from the full interaction operator. This can be done with the help of the two-phase orthogonalized model described in Sec. II. The exclusion of six-quark compound states can be conveniently accomplished by the well-known Feshbach formalism. This eventually leads to the Moscow-type models with its two orthogonal channels.

Our approach makes it possible to describe rather accurately both NN phase shifts up to 500 MeV, and the deuteron structure with a truncated one-pion exchange potential together with a simple deep *static* potential. Altogether we use six parameters with clear physical meaning. This evidently confirms the usefulness of the present two-phase approach. Other hybrid models which combine both quark- and meson-exchange degrees of freedom make use of *nonorthogonal* quark- and meson-exchange channels, i.e., some mixture of both. As a result, they contain *nontrivial* energy dependence and nonlocalities. In addition, most hybrid models do not offer a microscopic interpretation of the NN channel.

A clear separation of the nonpotential pieces of the NN interaction and the subsequent parametrization of the rest in an orthogonal *subspace* is the main physical idea underlying our approach. Therefore, the success of the model may be taken as some evidence for the formation of six-quark compound states (i.e., dibaryons) at short range in low partial waves. As a result of the elimination of $6q$-compound states, the $3N$, $4N$, and other many-nucleon systems are underbound.

In this work we have used only the one-phase *effective* two-body potential component of the complete two-phase model. In the future, it would be interesting to take the next step and to incorporate the second, i.e., $6q+N$ component in few- and many-body calculations. In addition, it would be interesting to include vector mesons into the theoretical description. Due to the additional orthogonality condition, their effect will not be as large as in standard force models, where the ωNN coupling constant is in contradiction with the SU(3) prediction [2]. In our case we are able to keep the ωNN coupling constant as low as SU(3) predicts.

ACKNOWLEDGMENTS

We are thankful to many of our colleagues in Moscow and Tübingen for long term fruitful discussions on the topics of the present study, especially to Professor E. W. Schmid, Professor V. G. Neudatchin, and Dr. I. T. Obukhovsky. One of the authors (V.I.K.) is very grateful to Professor Steven Moszkowski and Professor Gerry Brown for many useful comments on our approach. He is also grateful to Professor C. N. Yang, Head of the Theoretical Physics Institute at Stony Brook, for his invitation to the Institute. The Russian authors thank the Russian Foundation for Fundamental Research (Grant No. 96-02-18071) and the Deutsche Forschungsgemeinschaft (Grant No. Fa-67/20-1) for partial financial support.

[7]The M-type models presented here differ from the OCM approach by Saito [36] in a few essential aspects: our model is based on another, more convenient mathematical formalism that is used to incorporate the additional orthogonality conditions. Second, the physical meaning of the ''forbidden'' subspace is quite different in our case because we start from a two-phase interaction model. Third, we generally combine the (reduced) repulsive core and the additional orthogonality condition.

[1] G. E. Brown and A. D. Jackson, *The Nucleon-Nucleon Interaction* (North-Holland, Amsterdam, 1976).
[2] R. Machleidt, Karl Holinde, and Ch. Elster, Phys. Rep. **149**, 1 (1987); R. Machleidt, Adv. Nucl. Phys. **19**, 189 (1989).
[3] E. Hadjimichael, *International Review of Nuclear Physics* (World Scientific, Singapore, 1985), Vol. 3.
[4] G. Breit, M. H. Hull, K. E. Lassila, and K. D. Pyatt, Phys. Rev. **120**, 2227 (1960).
[5] M. Lacombe, B. Loiseau, J. M. Richard, R. Vinh Mau, J. Cote, P. Pires, and R. de Tourreil, Phys. Rev. C **21**, 861 (1980); Phys. Lett. **101B**, 139 (1981).
[6] H. Witala and W. Glöcke, Nucl. Phys. **A528**, 48 (1991): H. Witala, D. Hüber, and W. Glöckle, Phys. Rev. C **49**, R14 (1994).
[7] J. Strate *et al.*, J. Phys. G **14**, L229 (1988).
[8] W. Glöckle *et al.*, Few-Body Syst., Suppl. **9**, 34 (1995); A. Kievsky, *ibid.* **9**, 405 (1995).
[9] R. Machleidt, F. Sammarruca, and Y. Song, Phys. Rev. C **53**, R1483 (1996).
[10] R. Machleidt, in *Nuclear Reactions*, Vol. 2 of *Computational Nuclear Physics*, edited by K. Langanke *et al.* (Springer, New York, 1993) Chap. 1, pp. 1–29; J. L. Friar, G. L. Payne, V. G. J. Stoks, and J. J. de Swart, Phys. Lett. B **311**, 4 (1993).
[11] A. Faessler, F. Fernandez, G. Lübeck, and K. Shimizu, Phys. Lett. **112B**, 201 (1983); Nucl. Phys. **A402**, 555 (1983); Amand Faessler, Czech. J. Phys. **39**, 933 (1989).
[12] Amand Faessler, A. Buchmann, and Y. Yamauchi, Int. J. Mod. Phys. E **2**, 39 (1993); Y. Yamauchi, A. Buchmann, Amand Faessler, and A. Arima, Nucl. Phys. **A546**, 495 (1990).
[13] A. M. Kusainov, V. G. Neudatchin, and I. T. Obukhovsky, Phys. Rev. C **44**, 2343 (1991).
[14] L. S. Kisslinger, Phys. Lett. **112B**, 307 (1982).
[15] Yu. A. Simonov, Nucl. Phys. **A463**, 231c (1984); Yad. Fiz. **39**, 1542 (1983).
[16] M. Oka and K. Yazaki, Nucl. Phys. **A402**, 477 (1983); K. Bräuer, A. Faessler, F. Fernandez, and K. Shimizu, Z. Phys. A **320**, 609 (1985); S. Kuyucak and A. Faessler, Phys. Lett. **169B**, 128 (1986).
[17] F. Myhrer and J. Wroldsen, Rev. Mod. Phys. **60**, 629 (1988); Y. Yamauchi and M. Wakamatsu, Nucl. Phys. **A457**, 621 (1986).
[18] A. Valcarce, A. Buchmann, F. Fernandez, and Amand Faessler, Phys. Rev. C **50**, 2246 (1994); **51**, 1480 (1995).
[19] E. Lomon, J. Phys. (France) **46**, 232 (1985); P. Gonzalez, P. LaFrance, and E. Lomon, Phys. Rev. D **35**, 2142 (1987); P. LaFrance and E. L. Lomon, in *Proceedings of the International Conference on ''Mesons and Nuclei at Intermediate Energies,''* edited by M. Kh. Khankhasayev and Zh. B. Kurmanov (World Scientific, Singapore, 1995).
[20] V. I. Kukulin, in *Book of Contributions, 14th International YUPAP Conference on Few Body Problems in Physics*, Williamsburg, 1994 (unpublished), pp. 108–110.
[21] H. Feshbach, Ann. Phys. (N.Y.) **19**, 287 (1962).
[22] V. I. Kukulin, V. M. Krasnopolsky, and V. N. Pomerantsev, in *Proceedings Symposium on LIYaF Nucleon-nucleon and Hadron-nucleus Interactions at Intermediate Energies*, Leningrad, 1986 (unpublished), pp. 103–107.
[23] V. G. Neudatchin, I. T. Obukhovsky, V. I. Kukulin, and N. F. Golovanova, Phys. Rev. C **11**, 128 (1975).
[24] V. I. Kukulin and V. N. Pomerantsev, Ann. Phys. (N.Y.) **111**, 330 (1978).
[25] F. Michel and G. Reidemeister, Z. Phys. A **329**, 385 (1988).
[26] D. Baye, Phys. Rev. Lett. **58**, 2738 (1987).
[27] V. I. Kukulin and V. N. Pomerantsev, Prog. Theor. Phys. **88**, 159 (1992).
[28] S. Nakaichi-Maeda, Phys. Rev. C **51**, 1633 (1995).
[29] F. Tabakin, Phys. Rev. **174**, 1208 (1968).
[30] G. Racah, Rev. Mod. Phys. **21**, 494 (1949).
[31] M. Hamermesh, *Group Theory and Its Application to Physical Problems* (Addison-Wesley, Reading, MA, 1964).
[32] Fl. Stancu and L. Wilets, Phys. Rev. C **36**, 726 (1987).
[33] V. G. Neudatchin, Yu. F. Smirnov, and R. Tamagaki, Prog. Theor. Phys. **58**, 1072 (1977).
[34] I. T. Obukhovsky *et al.*, Phys. Lett. B **88**, 231 (1988).
[35] Amand Faessler, Chin. J. Phys. **29**, 533 (1991).
[36] S. Saito, Prog. Theor. Phys. **41**, 705 (1969); Nucl. Phys. **A472**, 161 (1987).
[37] L. Ya. Glozman, V. I. Kukulin, and V. N. Pomerantsev, Phys. Rev. C **45**, R17 (1992).
[38] V. I. Kukulin and V. N. Pomerantsev (unpublished).
[39] V. A. Matveev and P. Sorba, Lett. Nuovo Cimento **20**, 435 (1977); Nuovo Cimento A **45**, 257 (1978); H. Hogaasen, P. Sorba, and R. Viollier, Z. Phys. C **4**, 131 (1980).
[40] P. U. Sauer, *Proceedings of the International Conference on Few Body and Quark-Hadronic Systems*, Dubna, 1987 (unpublished), p. 188; M. M. Nagels, T. A. Rijken, and J. J. de Swart, Phys. Rev. D **17**, 768 (1978).
[41] R. A. Malfliet and T. A. Tjon, Nucl. Phys. **A127**, 161 (1969); Ann. Phys. (N.Y.) **61**, 425 (1970).
[42] P. U. Sauer, Phys. Rev. C **11**, 1786 (1975); in *Nucleon-Nucleon Interactions*, Vancouver, 1977, edited by D. F. Measday (AIP, New York, 1978), p. 195.
[43] S. Nakaichi-Maeda, Phys. Rev. C **34**, 303 (1986).
[44] K. Hahn, and P. Doleschall, and E. W. Schmid, Phys. Lett. **169B**, 118 (1986).
[45] H. Kamada (private communication).
[46] H. Leeb, H. Fiedeldey, and S. A. Sofianos, in [20], p. 125.
[47] V. I. Kukulin, V. M. Krasnopolsky, and V. N. Pomerantsev, in *Book of Contributions to the X International Conference Few Body Problems in Physics*, Karlsruhe, 1983 (unpublished), Chap. VII, p. 324.
[48] V. I. Kukulin, V. M. Krasnopolsky, V. N. Pomerantsev, and P. B. Sazonov, Phys. Lett. **135B**, 20 (1984): **165B**, 7 (1985).
[49] V. M. Krasnopolsky, V. I. Kukulin, and V. N. Pomerantsev, Izv. Akad. Nauk SSSR, Ser. Fiz. **51**, 898 (1987).
[50] V. I. Kukulin, V. M. Krasnopolsky, V. N. Pomerantsev, and P. B. Sazonov, Sov. J. Nucl. Phys. **43**, 559 (1986).
[51] V. I. Kukulin, Izv. Akad. Nauk SSSR, Ser. Fiz. **39**, 535 (1975).
[52] V. I. Kukulin and V. M. Krasnopolsky, J. Phys. G **3**, 795 (1977).
[53] H. Kameyama, M. Kamimura, and Y. Fukushima, Phys. Rev. C **40**, 974 (1989).
[54] S. Ishikawa and T. Sasakawa, Phys. Rev. C **36**, 2037 (1987).
[55] S. B. Dubovichenko, Yad. Fiz. **60**, 499 (1997).
[56] A. J. Buchmann, H. Henning, and P. U. Sauer, Few-Body Syst. **21**, 149 (1996).
[57] R. A. Arndt, *et al.*, *NN* phase shift analysis of 1995 (SM95), SAID (unpublished); R. A. Arndt, L. D. Roper, R. L. Workman, and M. W. McNaughton, Phys. Rev. D **45**, 3995 (1992).
[58] V. G. J. Stoks, R. A. M. Klomp, M. C. M. Rentmeester, and J. J. de Swart, Phys. Rev. C **48**, 792 (1993).
[59] V. I. Kukulin, V. G. Neudatchin, I. T. Obukhovsky, and Yu. F.

Smirnov, *Clusters as Subsystems in Light Nuclei* (Vieweg, Braunschweig, 1983).
[60] V. M. Krasnopolsky and V. I. Kukulin, Czech. J. Phys. **B27**, 290 (1977).
[61] F. P. Vasiliev, B. G. Kaganov, D. P. Kostomarov, and V. I. Kukulin, J. Comput. Math. Math. Phys., **28**, 1520 (1988).
[62] G. E. Brown and R. Machleidt, Phys. Rev. C **50**, 1731 (1997).
[63] R. A. Arndt *et al.*, Phys. Rev. D **28**, 97 (1983).
[64] R. B. Wiringa, Phys. Rev. C **43**, 1585 (1991); Ch. Hajduk and P. U. Sauer, Nucl. Phys. **A369**, 321 (1981).
[65] B. L. G. Bakker, *Proceedings. XII Few-Body European Conference*, Uzhgorod, USSR, 1990 (unpublished), p. 249.
[66] B. S. Pudliner, V. R. Pandharipande, J. Carlson, and R. B. Wiringa, Phys. Rev. Lett. **74**, 4396 (1995).
[67] M. Namiki, K. Okano, and N. Oshimo, Phys. Rev. C **25**, 2157 (1982).
[68] A. Amroun *et al.*, Nucl. Phys. **A579**, 596 (1994).
[69] V. G. Neudatchin, N. A. Khokholov, A. M. Shirokov, and V. A. Knyr, Phys. At. Nucl. **60**, 971 (1997).
[70] C. Ordonez, L. Ray, and U. van Kolck, Phys. Rev. C **53**, 2086 (1996).